



HHS Public Access

Author manuscript

Proc Int World Wide Web Conf. Author manuscript; available in PMC 2024 December 20.

Published in final edited form as:

Proc Int World Wide Web Conf. 2024 May ; 2024: 1170–1181. doi:10.1145/3589334.3645531.

DPAR: Decoupled Graph Neural Networks with Node-Level Differential Privacy

Qiuchen Zhang,

Emory University, Atlanta, GA, USA

Hong kyu Lee,

Emory University, Atlanta, GA, USA

Jing Ma,

Emory University, Atlanta, GA, USA

Jian Lou,

Zhejiang University, Hangzhou, China

Carl Yang,

Emory University, Atlanta, GA, USA

Li Xiong

Emory University, Atlanta, GA, USA

Abstract

Graph Neural Networks (GNNs) have achieved great success in learning with graph-structured data. Privacy concerns have also been raised for the trained models which could expose the sensitive information of graphs including both node features and the structure information. In this paper, we aim to achieve node-level differential privacy (DP) for training GNNs so that a node and its edges are protected. Node DP is inherently difficult for GNNs because all direct and multi-hop neighbors participate in the calculation of gradients for each node via layer-wise message passing and there is no bound on how many direct and multi-hop neighbors a node can have, so existing DP methods will result in high privacy cost or poor utility due to high node sensitivity. We propose a **D**ecoupled GNN with **D**ifferentially **P**rivate **A**pproximate **P**ersonalized **P**age**R**ank (DPAR) for training GNNs with an enhanced privacy-utility tradeoff. The key idea is to decouple the feature projection and message passing via a DP PageRank algorithm which learns the structure information and uses the top- K neighbors determined by the PageRank for feature aggregation. By capturing the most important neighbors for each node and avoiding the layer-wise message passing, it bounds the node sensitivity and achieves improved privacy-utility tradeoff compared to layer-wise perturbation based methods. We theoretically analyze the node

Permission to make digital or hard copies of all or part of this work for personal or classroom use is granted without fee provided that copies are not made or distributed for profit or commercial advantage and that copies bear this notice and the full citation on the first page. Copyrights for components of this work owned by others than the author(s) must be honored. Abstracting with credit is permitted. To copy otherwise, or republish, to post on servers or to redistribute to lists, requires prior specific permission and/or a fee. Request permissions from permissions@acm.org.

zhangqiuchen0929@gmail.com .

DP guarantee for the two processes combined together and empirically demonstrate better utilities of DPAR with the same level of node DP compared with state-of-the-art methods.

Keywords

Differential Privacy; Graph Neural Networks; PageRank

1 INTRODUCTION

Graph Neural Networks (GNNs) have shown superior performance in mining graph-structured data and learning graph representations for downstream tasks like node classification, link prediction, and graph classification [7, 19, 30, 41]. Like neural network models trained on private datasets that could expose sensitive training data, GNN models trained on graph data embedded with node features and topology are also vulnerable to various privacy attacks [40, 49, 50].

Differential privacy (DP) has become the standard for neural network training with rigorous protection for training data [1, 13]. A key method is DP stochastic gradient descent (DP-SGD) [1, 47], which introduces calibrated noise into gradients during SGD training. DP ensures a bounded risk for an adversary to deduce from a model whether a record was used in its training. For graph data, where both node features (e.g., personal attributes) and edges (e.g., social relationships) can be sensitive, our objective is to achieve node-level DP, limiting the risk of inferring whether a node and its edges were included in the training.

Challenges.

Achieving node DP for GNNs is inherently challenging. Unlike grid-based data such as images, graph data contains both feature vectors for each node and the edges that connect the nodes. During the training of GNN models, all direct and multi-hop neighbors participate in the calculation of gradients for each node via recursive layer-wise message passing [19, 41]. At each layer, each node aggregates the features (or the latent representations) from its neighbors when generating its own representation. There is no bound on how many direct and multi-hop neighbors a node can have. This means the sensitivity of the gradient due to the presence or absence of a node can be extremely high due to the node itself and its neighbors (or correlations between the nodes), which makes standard DP-SGD based methods [1, 46] infeasible, resulting in either high privacy cost or poor utility due to the large required DP noise.

Few recent works tackled node DP for training GNNs and they mainly attempted to bound the correlations during training to help bound the sensitivity or privacy cost. Daigavane et al. [9] sample subgraphs to ensure that each node has a bounded number of neighbors within each subgraph, and limit the occurrences of each node in other subgraphs such that it can apply the privacy-by-amplification technique [4, 23] to GNN. Their method is limited to GNNs with only one or two layers. The GAP algorithm [38] assumes a maximum degree for each node in order to bound the sensitivity of individual nodes. Meanwhile, their message-passing scheme requires DP noise at each step, therefore, it further bounds

the sensitivity by bounding the number of hops. This affects the model utility as it may restrict each node from acquiring useful information from higher hop neighbors. In sum, these approaches make it feasible to train GNNs with node DP but still sacrifice the model accuracy due to the restrictions on the number of hops during training.

Contributions.

We propose a Decoupled GNN with Differentially Private Approximate Personalized PageRank (DPAAPR, pronounced “dapper”) for training GNNs with node DP and enhanced privacy-utility tradeoff. The key idea is to decouple the feature aggregation and message passing into two processes: 1) use a DP Approximate Personalized PageRank (APPR) algorithm to learn the structure information, and 2) use the top- K neighbors determined by the APPR for feature aggregation and model learning with DP. In other words, the APPR learns the influence score of all direct and multi-hop neighbors, and the layer-wise message-passing is replaced by neighborhood aggregation based on the APPR.

Our framework is based on the decoupled GNN training frameworks [7, 25] which are originally designed to scale up the training for large graphs. Our main insight is that this decoupled strategy can be exploited to improve the design of DP algorithms. By capturing the most important neighbors for each node (bounding the node sensitivity) and avoiding the expensive privacy cost accumulation from the layer-wise message passing, our framework achieves enhanced privacy-utility tradeoff compared to layer-wise perturbation based methods.

Adding DP to this decoupled framework is nontrivial and presents several challenges. First, there are no existing works for computing sparsified APPR with formal node DP. While there exist DP top- K selection algorithms [12], directly applying it can result in poor accuracy due to high sensitivity since each node (and its edges) can affect all the elements in the APPR matrix. Second, while DP-SGD can be used for feature aggregation, the neighborhood sampling returns a correlated batch of nodes based on the APPR, making the privacy analysis more complex, particularly for quantifying the privacy amplification ratio. To address these challenges, we develop DP-APPR algorithms to compute the top- K sparsified APPR with DP. We then utilize DP-SGD [1] for feature aggregation and model training to protect node features. We analyze the privacy loss caused by the neighborhood sampling and calibrate tighter Gaussian noise for the clipped gradients to provide a rigorous overall privacy guarantee. We summarize our contributions as follows.

- We propose DPAAPR, a novel de-coupled DP framework with sparsification for training GNNs with rigorous node DP. DPAAPR decouples message passing from feature aggregation via DP APPR and uses the top- K neighbors determined by APPR for feature aggregation, which captures the most important neighbors for each node and avoids the layer-wise message passing and achieves better privacy-utility tradeoff than existing layer-wise perturbation based methods.
- We develop two DP APPR algorithms based on the exponential mechanism and Gaussian mechanism for selecting top- K elements in the APPR vector with formal node DP. We employ sampling and clipping to address the high sensitivity challenge. We utilize the exponential mechanism [12, 13] to select the indices of

the top- K elements first, and then compute the corresponding noisy values with additional privacy costs. Alternatively, the Gaussian mechanism directly adds noise to the APPR vector and then selects the top- K from the noisy vectors. We formally analyze the privacy guarantee for both methods.

- We use DP-SGD for feature aggregation and model learning based on the DP APPR. By using the top- K sparsified DP APPR vectors, we limit the maximum number of nodes one node can affect during gradient computation, which is the maximum column-wise ℓ_1 norm of the DP APPR matrix. We incorporate additional clipping to ensure a maximum ℓ_1 norm per column which determines the sensitivity of each node. We calibrate the Gaussian noise by theoretically analyzing the privacy loss and privacy amplification caused by the neighborhood sampling determined by the DP APPR and provide a rigorous privacy guarantee for DPAR.
- We conduct extensive experiments on five real-world graph datasets to evaluate the effectiveness of the proposed algorithms. Results show that they achieve better accuracy at the same level of node DP compared to the state-of-the-art algorithms. We also illustrate the privacy protection of the trained models.

2 BACKGROUND

2.1 GNNs with Personalized PageRank

Given a graph $G = (V, E, X)$, where V and E denote the set of vertices and edges, respectively, and $X \in \mathbb{R}^{|V| \times d}$ represents the feature matrix where each row corresponds to the associated feature vector $X_v \in \mathbb{R}^d (v = 1, \dots, |V|)$ of node v . Each node is associated with a class (or label) vector $Y_v \in \mathbb{R}^c$, such as the one-hot encoding vector, with the number of classes c . Considering the node classification task as an instance, a GNN model learns a representation function f that generates the node embedding h_v for each node $v \in V$ based on the features of the node itself as well as all its neighbors [41], and the generated node embeddings will further be used to label the class of unlabeled nodes using the softmax classifier with the cross-entropy loss.

GNN models use the recursive message-passing procedure to spread information through a graph, which couples the neighborhood aggregation and feature transformation for node representation learning. This coupling pattern can cause some potential issues in model training, including neighbor explosion and over-smoothing [7, 30]. Recent works propose to decouple the neighborhood aggregation process from feature transformation and achieve superior performance [7, 11]. Bojchevski et al. [7] show that neighborhood aggregation/propagation based on personalized PageRank [18] can maintain the influence score of all “neighboring” (relevant) nodes that are reachable to the source node in the graph, without the explicit message-passing procedure. They pre-compute a pagerank matrix Π and truncate it by keeping only the top k largest entries of each row and setting others to zero to get a sparse matrix Π^{PPR} , which is then used to aggregate node representations, generated using a

neural network, of “neighbors” (most relevant nodes) to get final predictions, expressed as follows:

$$z_v = \text{softmax}\left(\sum_{u \in \mathcal{N}^k(v)} \pi'(v)_u H_{u,:}\right), \quad (1)$$

where $\mathcal{N}^k(v)$ enumerates indices of the k non-zero entries in $\pi'(v)$ which is the v -th row of $\mathbf{\Pi}^{PPR}$ corresponding to the node v 's sparse APPR vector. $H_{u,:}$ is the node representation generated by a neural network f_θ using the node feature vector X_u of each node u independently.

2.2 Differential Privacy (DP)

DP [13, 34] has demonstrated itself as a strong and rigorous privacy framework for aggregate data analysis in many applications. DP ensures the output distributions of an algorithm are indistinguishable with a certain probability when the input datasets differ in only one record.

DEFINITION 1. ((ϵ, δ) -Differential Privacy) [13]. *Let \mathcal{D} and \mathcal{D}' be two neighboring datasets that differ in at most one entry. A randomized algorithm \mathcal{A} satisfies (ϵ, δ) -differential privacy if for all $\mathcal{S} \subseteq \text{Range}(\mathcal{A})$:*

$$\Pr[\mathcal{A}(\mathcal{D}) \in \mathcal{S}] \leq e^\epsilon \Pr[\mathcal{A}(\mathcal{D}') \in \mathcal{S}] + \delta,$$

where $\mathcal{A}(\mathcal{D})$ represents the output of \mathcal{A} with the input \mathcal{D} , ϵ and δ are the privacy parameters (or privacy budget) and a lower ϵ and δ indicate stronger privacy and lower privacy loss.

In this paper, we aim to achieve node-level DP for graph data to protect both the features and edges of a node.

DEFINITION 2. ((ϵ, δ) -Node-level Differential Privacy) *Let \mathcal{G} and \mathcal{G}' be two neighboring graphs that differ in at most one node including its feature vector and all its connected edges. A randomized algorithm \mathcal{A} satisfies (ϵ, δ) -node-level DP if for all $\mathcal{S} \subseteq \text{Range}(\mathcal{A})$:*

$$\Pr[\mathcal{A}(\mathcal{G}) \in \mathcal{S}] \leq e^\epsilon \Pr[\mathcal{A}(\mathcal{G}') \in \mathcal{S}] + \delta,$$

where $\mathcal{A}(\mathcal{G})$ represents the output of \mathcal{A} with the input graph \mathcal{G} .

2.3 DP-SGD and Challenges

A widely used technique for achieving DP for deep learning models is DP stochastic gradient descent (DP-SGD) algorithm [1, 26]. It first computes the gradient $\mathbf{g}(x_i)$ for each example x_i in the randomly sampled batch with size B , and then clips the ℓ_2 norm of each gradient with a clipping threshold C to bound the sensitivity of $\mathbf{g}(x_i)$ to C . The clipped gradient $\bar{\mathbf{g}}(x_i)$ of each example will be summed together and added with the Gaussian noise

$\mathcal{N}(0, \sigma^2 C^2 \mathbf{I})$ to protect privacy. Finally, the average of the noisy accumulated gradient $\tilde{\mathbf{g}}$ will be used to update the model parameters for this step. We express $\tilde{\mathbf{g}}$ as:

$$\tilde{\mathbf{g}} \leftarrow \frac{1}{B} \left(\sum_{i=1}^B \bar{\mathbf{g}}(x_i) + \mathcal{N}(0, \sigma^2 C^2 \mathbf{I}) \right). \quad (2)$$

In DP-SGD, each example individually calculates its gradient, e.g., only the features of x_i will be used to compute the gradient $\mathbf{g}(x_i)$ for x_i . However, when training GNNs, nodes are no longer independent, and one node's feature will affect the gradients of other nodes. In a GNN model with K layers, one node has the chance to utilize additional features from all its neighbors up to K -hop when calculating its gradient. Rethinking Equation 2, the bound of the sensitivity of $\sum_{i=1}^B \bar{\mathbf{g}}(x_i)$ becomes $B * C$ since changing one node could potentially change the gradients of all nodes in the batch $\sum_{i=1}^B \bar{\mathbf{g}}(x_i)$. Substituting $B * C$ for C in Equation 2 and we get the following equation:

$$\tilde{\mathbf{g}} \leftarrow \frac{1}{B} \left(\sum_{i=1}^B \bar{\mathbf{g}}(x_i) + \mathcal{N}(0, \sigma^2 B^2 C^2 \mathbf{I}) \right). \quad (3)$$

Comparing Equation 3 to 2, to achieve the same level of privacy at each step during DP-SGD, the standard deviation of the Gaussian noise added to the gradients is scaled up by a factor of the batch size B , resulting in poor utility. Existing works [9, 38] mitigate the high sensitivity by bounding the number of hops and node degrees but also sacrifice the information that can be learned from higher hop neighbors, resulting in limited success in improving accuracy.

3 DPAR

We present our DPAR framework for training DP GNN models via DP approximate personalized PageRank (APPR). The key idea is to exploit the decoupled framework (Section 2.1) and decouple message passing from feature aggregation into two steps: 1) use a DP APPR algorithm to learn the structure information (Section 3.1), and 2) use the top- K neighbors determined by the APPR for feature aggregation and model learning with DP-SGD (Section 3.2). By capturing the most important neighbors for each node from the APPR and avoiding explicit message passing, it bounds the node sensitivity without sacrificing model accuracy, achieving an improved privacy-utility tradeoff. The overall privacy budget will be split between the two steps, and we theoretically analyze the node DP guarantee for the entire framework in Section 3.2.

3.1 Differentially Private APPR

We develop our DP APPR algorithms based on the ISTA algorithm [15] for computing APPR. Andersen et al. [3] proposed the first approximate personalized PageRank (APPR) algorithm which is adopted in [7, 25] to replace the explicit message-passing procedure for GNNs. Most recently, Fountoulakis et al. [15] demonstrated that the APPR algorithm

can be characterized as an ℓ_1 -regularized optimization problem, and proposed an iterative shrinkage-thresholding algorithm (ISTA) (Algorithm 3 in [15]) to solve it with a running time independent of the size of the graph. The input of ISTA contains the adjacency matrix of a graph and the one-hot vector corresponding to the index of one node in the graph, and the output is the APPR vector of that node. We develop our DP APPR algorithm based on ISTA due to its status as one of the state-of-the-art APPR algorithms. ISTA provides an excellent balance between scalability and approximation guarantees. Moreover, the resulting sparse APPR matrix can be easily accommodated into the memory, facilitating the subsequent neural network training.

Recall the purpose of calculating APPR vectors is to utilize them to aggregate representations from relevant nodes for the source node during model training. The index of each entry in an APPR vector indicates the index of a node in the graph, and the value of each entry reflects the importance or relevance of this node to the source node. By reserving the top K largest entries for each APPR vector, the feature aggregation step computes a weighted average of the representations of the K most relevant nodes to the source node (recall Equation 1). The graph structure information is encoded in both the indexes and values of non-zero entries in each sparse APPR vector. Thus, to provide DP protection for the graph structure, we propose two DP APPR algorithms to obtain the top- K indexes and values for each APPR vector.

Algorithm 1: DP-APPR using the Exponential Mechanism (DP-APPR-EM)

Input: ISTA hyperparameters: γ, α, ρ ; privacy parameters: $\epsilon, \epsilon_2, \delta$; clip bound C_2 , a graph (V, E) where $V = \{v_1, \dots, v_N\}$, an integer $K > 0$ and an integer $M \in [1, N]$.

- 1 Initialize the APPR matrix $\Pi \in \mathbb{R}^{M \times N}$ with all zeros.
- 2 for $i = 1, \dots, M$ do
- 3 **Compute APPR:**
- 4 Compute the APPR vector $\mathbf{p}_{(v_i)}$ for node v_i using ISTA;
- 5 **Clip Norm:**
- 6 $\hat{\mathbf{p}}_{(v_i)} \leftarrow$: for each entry $\mathbf{p}_{(v_i)}[j], j \in [1, \dots, N]$, set $\mathbf{p}_{(v_i)}[j] = \mathbf{p}_{(v_i)}[j] / \max\left(1, \frac{\|\mathbf{p}_{(v_i)}\|_1}{C_2}\right)$
- 7 **Add Noise:**
- 8 $\tilde{\mathbf{p}}_{(v_i)} \leftarrow \hat{\mathbf{p}}_{(v_i)} + \text{Gumbel}(\beta \mathbf{1})$, where $\beta = C_2 / \epsilon$;
- 9 **Report Noisy Indexes:**
- 10 $N_K \leftarrow$: select the indexes of the top K entries with the largest values in $\tilde{\mathbf{p}}_{(v_i)}$;
- 11 **Report Noisy Values:**
- 12 option I: $\tilde{\mathbf{p}}'_{(v_i)} \leftarrow$: set $\tilde{\mathbf{p}}_{(v_i)}[j], j \in N_K$, to be $1/K$, and other entries to be 0;
- 13 option II: $\tilde{\mathbf{p}}'_{(v_i)} \leftarrow$: set $\tilde{\mathbf{p}}_{(v_i)}[j], j \in N_K$, to be $\tilde{\mathbf{p}}_{(v_i)}[j] + \text{Laplace}(KC_2/\epsilon_2)$, and other entries to be 0;
- 14 **Replace** the i -th row of Π with $\tilde{\mathbf{p}}'_{(v_i)}$.
- 15 end
- 16 return Π and the overall privacy cost.

Exponential Mechanism (DP-APPR-EM).—We present the DP APPR algorithm using the exponential mechanism. While we can employ a DP top- K selection algorithm based on the exponential mechanism [12], there are several challenges that need to be addressed. First, each node (and its edges) can change an arbitrary number of elements in the APPR vector and lead to significant changes in each element. Second, each node can change an

arbitrary number of APPR vectors in the APPR matrix. Both of these mean extremely high sensitivity, making a direct application of the top- K selection algorithm ineffective. To address them, we employ two techniques: 1) clipping each element to bound the sensitivity, 2) sampling and only computing APPR for a subset of M nodes in the graph to reduce sensitivity. We then employ the exponential mechanism to select the top- K values.

As shown in Algorithm 1, for each of the M sampled nodes, we first compute the APPR vector using the ISTA algorithm (line 4). Then we employ clipping to bound the sensitivity of each element by C_2 (line 6). We use the clipped value as its utility score for the exponential mechanism since the magnitude of each entry indicates its importance (utility) and is used as the weight when aggregating the representation of the nodes. We simulate the exponential mechanism by injecting a one-shot Gumbel noise to the clipped vector $\hat{\mathbf{p}}_{(v)}$ (line 8) and then select the indexes of top K largest noisy entries [12] (line 10). We can then either: option I) set the values of all top K entries to be $1/K$ (line 12), which means we consider the top K entries equally important to the source node, or option II) spend additional privacy budget ϵ_2 to obtain the noisy values of the top K entries with DP (line 13). Given the same privacy budget, the option I has a better chance to output indexes of the actual top K entries while losing the importance scores. In contrast, option II sacrifices some accuracy in selecting the indexes of top K entries but has additional importance scores.

Privacy Analysis of DP-APPR-EM.—We formally analyze the DP guarantee of Algorithm 1 utilizing the following corollary for the exponential mechanism based top- K selection.

COROLLARY 1. [12] $\mathcal{M}_{\text{Gumbel}}^k(u)$ adds the one-shot Gumbel($\Delta(u)/\epsilon$) noise to each utility score $u(x, r)$ and outputs the k indices with the largest noisy values. For any $\delta \geq 0$, $\mathcal{M}_{\text{Gumbel}}^k(u)$ is (ϵ', δ) -DP where

$$\epsilon' = 2 \cdot \min \left\{ k\epsilon, k\epsilon \left(\frac{e^{2\epsilon} - 1}{e^{2\epsilon} + 1} \right) + \epsilon \sqrt{2k \ln(1/\delta)} \right\}$$

The privacy analysis conducted in [12] assumes independent users and the sensitivity $\Delta(u)$ is 1. In our case, each node (and its edges) can modify an arbitrary number of elements in the APPR vector and each element can change at most by C_2 due to clipping (line 6). Consequently, the sensitivity $\Delta(u)$ used in Corollary 1 is set to C_2 and the noise is calibrated accordingly in our algorithm (line 8). Additionally, since each node can change up to M vectors in the APPR matrix, we use sequential composition to bound the privacy loss for M APPR vectors. With the calibrated noise and composition, we establish the DP guarantee in Theorem 1.

THEOREM 1. For any $\epsilon > 0$, $\epsilon_2 > 0$ and $\delta \in (0, 1]$, let $\epsilon_1 = 2 \cdot \min \left\{ K\epsilon, K\epsilon \left(\frac{e^{2\epsilon} - 1}{e^{2\epsilon} + 1} \right) + \epsilon \sqrt{2K \ln(1/\delta)} \right\}$, Algorithm 1 is $(\epsilon_{s_1}, 2M\delta)$ -differentially private for option I, and $(\epsilon_{s_2}, 2M\delta)$ -

differentially private for option II, where $\epsilon_1 = \epsilon_{g_1}/(2\sqrt{M \ln(e + \epsilon_{g_1}/2M\delta)})$ and $\epsilon_1 + \epsilon_2 = \epsilon_{g_2}/(2\sqrt{M \ln(e + \epsilon_{g_2}/2M\delta)})$.

PROOF. See Appendix A for the proof.

Gaussian Mechanism.—We explore another DP-APPR algorithm (DP-APPR-GM) based on Gaussian mechanism [13] and output perturbation. The idea behind DP-APPR-GM is to use the clipping strategy to bound the global sensitivity of each output PageRank vector and add Gaussian noise to each bounded PageRank vector to achieve DP. See Appendix B for more details about DP-APPR-GM.

3.2 Differentially Private GNNs

We show our overall approach for training a DP GNN model in Algorithm 2. The main idea is to use DP APPR for neighborhood sampling and then use DP-SGD to achieve DP for the node features. We employ additional sampling and clipping to reduce the privacy cost.

Algorithm 2: Differentially Private GNNs

Input: The graph dataset \bar{G} , sampling rate q' , randomly sampled training graph $G = (V, E, X)$ from \bar{G} by q' where $V = \{v_1, \dots, v_N\}$, a sampled subset $V_M \subseteq V$ with size M (for computing APPR), learning rate η_t , batch size B , training steps T , noise scale σ , gradient norm bound C , clip bound τ , the DP APPR matrix $\Pi \in \mathbb{R}^{M \times N}$ of V_M satisfying $(\epsilon_{pr}, \delta_{pr})$ -DP.

- 1 Initialize θ_0 randomly
- 2 for $j = 1, \dots, N$ do
- 3 $\Pi_{:,j} \leftarrow \Pi_{:,j} / \max\left(1, \frac{\|\Pi_{:,j}\|_1}{\tau}\right)$
- 4 end
- 5 for $t = 1, \dots, T$ do
- 6 Take a randomly sampled batch B and their K neighbors based on Π from V_M .
- 7 **Compute Gradient:**
- 8 For each $i \in B_t$, compute $g_t(v_i) \leftarrow \nabla_{\theta_t} \mathcal{L}(\theta_t, v_i)$.
- 9 **Clip Gradient:**
- 10 $\bar{g}_t(v_i) \leftarrow g_t(v_i) / \max\left(1, \frac{\|g_t(v_i)\|_2}{C}\right)$.
- 11 **Add Noise:**
- 12 $\tilde{g}_t \leftarrow \frac{1}{B} (\sum_i \bar{g}_t(v_i) + \mathcal{N}(0, \sigma^2 C^2 \mathbf{1}))$.
- 13 **Update Parameters:**
- 14 $\theta_{t+1} \leftarrow \theta_t - \eta_t \tilde{g}_t$.
- 15 end
- 16 return θ_T and the overall privacy cost.

Given a graph dataset \bar{G} , we first use a sampling rate q' to randomly sample nodes from \bar{G} to form a subgraph $G = (V, E, X)$ containing only the sampled nodes and their connected edges, which is used for training in Algorithm 3. This sampling step brings a privacy amplification effect in our privacy guarantee by a factor of [5, 23]. Note that this is different from the batch sampling during each iteration of the training process. We further sample M nodes to compute the DP APPR using DP-APPR-EM or DP-APPR-GM and use it as input for Algorithm 2.

Utilizing the sparsified DP APPR vectors (each row has only top- K non-zero elements) limits the impact of a node on the gradient computation of up to B' nodes, where B' is the

maximum column-wise ℓ_0 norm of the DP APPR matrix (number of non-zero elements in each column). The exact impact or sensitivity is determined by the maximum column-wise ℓ_1 norm of the DP APPR matrix (see privacy analysis for more details). Hence, we employ additional clipping on the DP APPR matrix to bound the sensitivity. Given Π computed using DP-APPR algorithms, each column of Π is clipped to have a maximum ℓ_1 norm of τ to limit privacy loss (line 3).

During each training step, we sample a batch of B nodes and their top- K neighbors (both direct and indirect) using APPR vectors, loading features of up to $B \times K$ nodes for gradient computation (line 6). The loss function $\mathcal{L}(\theta, v_i)$ is the cross-entropy between node v_i 's true label and its prediction from Equation 1. Following DP-SGD, we compute each node's gradient, clip it to a maximum ℓ_2 norm of C , and introduce Gaussian noise with sensitivity C (line 7 – 12). The model is updated with the averaged noisy gradient (line 14).

Privacy Analysis.—Theorem 2 presents the DP analysis of Algorithm 2. An essential distinction between our algorithm and the original DP-SGD is that our neighborhood sampling returns a correlated batch of nodes for gradient computation (i.e., the computation of $\mathbf{g}(v_i)$ requires the features of the neighboring nodes of node v_i , and node v_i accesses the fixed K nodes based on the DP-APPR vector), while the original DP-SGD uses the much simpler Poisson sampling. As a result, the privacy analysis of our algorithm is more involved, especially in terms of quantifying the privacy amplification ratio under such a neighbor-correlated sampling setting. We prove that the privacy amplification ratio is proportional to the maximum of the column-wise ℓ_1 norm of the DP-APPR matrix.

For the composition of DP-APPR and DP-SGD, we use the standard composition theorem. Recall that for the privacy composition of multiple DP-APPR vectors for the DP-APPR matrix (Theorem 1 and 2), we used a strong composition theorem. We note that our privacy analysis can always benefit from a more advanced composition theorem to achieve tighter overall privacy, which can be a future work direction.

THEOREM 2. *There exist constants c_1 and c_2 so that given probability $q = B/N$ and the number of steps T , for any $\epsilon_{sgd} < c_1 q^2 T$, Algorithm 2 is $q'(\epsilon_{sgd} + \epsilon_{pr}, \delta_{sgd} + \delta_{pr})$ -differentially private corresponding to \bar{G} , for any $\delta_{sgd} > 0$ if we choose $\sigma \geq c_2 \frac{q\tau\sqrt{T\log(1/\delta_{sgd})}}{\epsilon_{sgd}}$.*

PROOF. See Appendix C for the proof.

4 EXPERIMENTAL RESULTS

We evaluate our method on five graph datasets with varying sizes and edge density: Cora-ML [6], Microsoft Academic graph [39], CS [39], Physics [39], and Reddit [19]. Appendix D provides the details of each dataset.

Setup.

To simulate the real-world situations where training nodes are assumed to be private and not publicly available, we split the nodes into a training set (80%) and a test set (20%), and select

inductive graph learning setting by removing edges between the two sets. The training nodes are inaccessible during inference. We use the same 2-layer feed-forward neural network with a hidden layer size of 32 as in [7] for all datasets. The training epochs are fixed at 200, the learning rate at 0.005, and the batch size at 60. The hyperparameters for ISTA are chosen through grid search as $\alpha = 0.25$, $\rho = 10^{-4}$, and $\gamma = 10^{-4}$. In our comparison with baseline methods, we set K to 2 for computing top- K sparsified DP APPR. We also present results on the effect of K with different K values. The graph sampling rate is set to $q' = 9\%$ for all datasets, and $M = 70$ nodes are chosen randomly and uniformly to generate DP-APPR vectors. Experiments are conducted on a server with an Nvidia K80 GPU, a 6-core Intel CPU, and 56 GiB RAM. Results are based on the mean of 10 independent trials. The source code is available¹.

Our Approach and Baselines.

Our proposed algorithms using the DP-APPR with exponential mechanism (options I and II in Algorithm 1) are referred to as **DPAR-EM0** and **DPAR-EM1**, respectively, and our algorithm using the DP-APPR with Gaussian mechanism is referred to as **DPAR-GM**.

We compare our proposed algorithms with two state-of-the-art methods achieving node DP for GNN and one baseline method: 1) **SAGE** [9] samples subgraphs of 1-hop neighbors of each node to train 1-layer GNNs with the GraphSAGE [19] model. 2) **GAP** [38] uses aggregation perturbation and MLP-based encoder and classifier with DP-SGD and a bounded node degree and number of hops. 3) **Features** is a baseline method that only uses node feature as an independent input to train the GNN model and does not consider the structural information of the graph. **Features** utilizes the original DP-SGD to achieve node DP. Note that it is equal to the case where we use a one-hot vector as each node's APPR vector in Algorithm 2 (i.e., no correlation with other nodes is used). We included this baseline to help characterize the datasets and calibrate the results, i.e., a good performance of the method may suggest that the topological structure of the particular dataset has limited benefit in training GNN. The models **DPARN_oDP** and **GAPN_oDP** indicate the respective methods (**DPAR**, **GAP**) with no DP protection.

Inference Phase.

As suggested in [7], instead of computing the APPR vectors for all testing nodes and generating predictions based on their APPR vectors, we use power iteration during inference:

$$Q^{(0)} = H, \quad Q^{(p)} = (1 - \alpha)D^{-1}AQ^{(p-1)} + \alpha H, \quad p \in [1, \dots, P]. \quad (4)$$

where H is the representation matrix of testing nodes generated by the trained private model, with the input being the feature matrix of the testing nodes; D and A are the degree matrix and adjacency matrix of the graph containing only testing nodes, respectively. The final

¹The source code is available at: <https://github.com/Emory-AIMS/DPAR>.

output of power iteration $Q^{(P)}$ will be input into a softmax layer to generate the predictions for testing nodes. We set $P = 2$ and the teleportation constant $\alpha = 0.25$ as suggested in [7] in our experiments.

4.1 Privacy vs. Accuracy Trade-off

We use the value of privacy budget ϵ (with fixed δ chosen to be roughly equal to the inverse of each dataset's number of training nodes) to represent the level of privacy protection and use the test accuracy for node classification to indicate the model's utility. Table 1 shows the results of our proposed methods and the baselines in all datasets, where the total privacy budget is evenly divided between DP-APPR and DP-SGD. In comparison to **GAP** and **SAGE**, our methods show superior test accuracy under the same privacy budget on all datasets. For instance, when $\epsilon = 1$, our methods (**DPAR-GM**, **DPAR-EM0**, or **DPAR-EM1**) achieve the highest test accuracy of 0.3421/0.8569/0.8927/0.934/0.8948 on Cora-ML/MS Academic/CS/Reddit/Physics datasets respectively. The best accuracy achieved by the baselines (**GAP** or **SAGE**) is 0.34/0.6563/0.66/0.7047/0.8192 on the corresponding datasets, indicating a test accuracy improvement by 0.62%/30.6%/35.3%/32.5%/9.23% respectively. The performance improvement demonstrates our method's superior ability to balance the privacy-utility trade-off on training graph datasets with privacy considerations.

Existing research in the graph neural network community suggests that features alone, especially for heterophilic graphs, can sometimes result in better-trained node classification models with MLP as the backend architecture compared to state-of-the-art GNN models [35]. For the Cora-ML dataset, which has a low edge density, the **Features** approach outperforms our methods when ϵ is small (e.g., 1). This is because our methods allocate part of the privacy budget to protect graph structure information, which may not be as critical, while **Features** uses its entire privacy budget to protect node features without considering graph structure information. However, as ϵ increases (e.g., 8), our methods outperform **Features**.

Our proposed methods protect the graph structure and node features independently via the decoupled framework. Different graphs possess unique characteristics, and the relative significance of structure information and node features can differ among them. Accordingly, our methods are able to allocate the total privacy budget differently to protect node features and structures, which leads to more precise and tunable privacy protection for graph data that includes both feature and structural information.

Ablation Study of Different DP-APPR Methods.—To further study the impact of DP-APPR on the model accuracy, in Figure 1, we fix ϵ_{sgd} (privacy budget for DP-SGD) and use varying ϵ_{pr} (privacy budget for DP-APPR) as the x-axis. For **DPAR-GM** and **DPAR-EM1**, the higher the ϵ_{pr} , the less noise is added when calculating the APPR vector for each training node. This allows a better chance for each node to aggregate representations from more important nodes using more precise importance scores. Hence these models have higher test accuracy compared to **DPAR-EM0**. In contrast, for **DPAR-EM0**, noise in DP-APPR will only affect the output of the indexes of the top- K most relevant nodes corresponding to the source node, but not their importance scores. **DPAR-EM0** achieves better performance

than **DPAR-GM** and **DPAR-EM1** when the privacy budget ϵ_p is small, this is because **DPAR-EM0** uses $1/K$ as the importance score for all nodes (considering nodes equally important), which diminishes the negative effect of less important or irrelevant nodes having high importance scores due to the noise in **DPAR-GM** and **DPAR-EM1**. Both **DPAR-EM0** and **DPAR-EM1** are based on the exponential mechanism designed for identifying the index of the top- K accurately. Therefore, when the privacy budget is small, they outperform **DPAR-GM**. However, when the privacy budget is large, they all have a good chance to find the indexes of the actual top- K , and **DPAR-GM** becomes gradually better than **DPAR-EM0** and **DPAR-EM1**, as the Gaussian noise has better privacy loss composition property.

4.2 Privacy Protection Effectiveness

Privacy Budget Allocation between DP-APPR and DP-SGD.—The total privacy budget is divided between DP-APPR and DP-SGD. We compare the impact of the budget allocation by changing the ratio of the total privacy budget used by each of them. Figure 2, 3, 4, 5, and 6 report the model test accuracy with varying ratios of the total privacy budget used for DP-APPR for the five datasets respectively, and they share the same legend as in Figure 2. A lower ratio means a smaller privacy budget is allocated for DP-APPR while more is allocated for DP-SGD. The impact of the ratio on the privacy-utility trade-off is closely aligned with the characteristics of each dataset. From Figure 2, the model achieves better accuracy when the ratio is lower, regardless of the total privacy budget. This is because of the characteristics of the Cora-ML dataset, as its node features are more important than its structure. Interestingly, when the privacy budget is small, Figure 3, 4, 5, and 6 show that information from node features is crucial for all datasets. Allocating more privacy budget to DP-SGD can learn more useful information from the node features and improve model accuracy. When the privacy budget is large, e.g., $\epsilon = 8$, we find that in MS Adademic and CS datasets, the model can achieve the best results when the budget is equally divided, suggesting the importance of learning from both the structure information and features.

4.3 Effects of Privacy Parameters

We use the Cora-ML dataset as an example to demonstrate the effects of the parameters specific to privacy, including the clipping bound in DP-APPR, the number of nodes M in DP-APPR, the number of selected top- K entries in DP-APPR, the batch size in DP-SGD, and the clipping bound in DP-SGD. By default, we set the batch size to 60, the clipping bound C_1 in DP-APPR-GM (Algorithm 3 in Appendix) to 0.01, the clipping bound C_2 in DP-APPR-EM (Algorithm 1) to 0.001, the gradient norm clipping bound C for DP-SGD to 1, and M to 70. We analyze them individually while keeping the rest constant as the default values.

Clipping Bound in DP-APPR (C_1 and C_2).—Figure 7 shows the effect of clipping bound in DP-APPR on the model's test accuracy. Given a constant total privacy budget, the standard deviation of the noise added to the APPR vectors is proportional to the clipping bound (C_1 in DP-APPR-GM and C_2 in DP-APPR-EM). Hence, choosing a smaller clipping bound in general can avoid adding too much noise and result in better accuracy. However,

too small of a clipping bound may degrade the accuracy due to the clipping error. In experiments, we set C_1 to be 0.01 and C_2 to be 0.001 for all datasets.

Number of Top- K in DP-APPR (K).—Figure 8 shows the accuracy with respect to varying $K(2, 4, 8, 16, 32)$ for the top- K selection in DP-APPR. The Gaussian mechanism’s sensitivity depends on the ℓ_2 norm of the APPR vector. We use a clip bound C_1 to restrict the ℓ_2 norm of the APPR vector, therefore the privacy guarantees are linked to C_1 , not K . K impacts the number of non-zero entries in each DP-APPR vector, influencing node feature embeddings. A small K may not capture enough neighbors while a higher K may include more irrelevant nodes as “neighbors”, adversely affecting aggregated information. For the Exponential mechanism, we clip each APPR vector value by C_2 to control sensitivity. The privacy guarantee is dependent on both C_2 and K . A larger K means more noise for each entry, affecting accuracy. From Figure 8, we can observe that DPAR-EM1 results highlight this effect, while DPAR-EM0 mitigates it by assigning a value of $1/K$ without additional noise. In our experiments compared against baselines, we use a fixed $K = 2$ for all datasets.

We also investigate the impact of batch size in DP-SGD (B), the clipping bound in DP-SGD (C), and the number of nodes in DP-APPR (M). We have included the results in Appendix F.

5 RELATED WORK

Differentially Private Graph Publishing.

Works on privacy-preserving graph data publishing aim to release the entire graph [17, 21, 36, 42], or the statistics or properties of the original graph [2, 8, 10, 24, 32, 44], with the DP guarantee. Different from those works, our work focuses on training GNN models on private graph datasets and publishing the model that satisfies node-level DP.

Differentially Private Graph Neural Networks.

Yang et al. [43] propose using DP-SGD to train a graph generation model with edge-DP, protecting link privacy. Sajadmanesh et al. [37] develop a GNN training algorithm based on local DP (LDP) to protect node features’ privacy, excluding edge privacy. Zhang et al. [48] apply LDP and the functional mechanism [45] to secure user’s sensitive features in graph embedding models for recommendations. Lin et al. [29] suggest a privacy-preserving framework for decentralized graphs, ensuring LDP on edge DP for each user. Epasto et al. [14] introduce a DP Personalized PageRank algorithm with edge-level DP for graph embedding. These efforts do not provide strict node-level DP for features and edges in GNN model training. Few recent works [9, 38] achieve node-level DP for GNNs, yet compromise model accuracy due to training restrictions on hops or layers. Our results show DPAR outperforms these methods.

6 CONCLUSION

We addressed private learning for GNN models with a two-stage framework: DP approximate personalized PageRank (DP-APPR) and DP-SGD, safeguarding graph structure and node features respectively. We developed two DP-APPR algorithms using Gaussian and

exponential mechanisms to learn PageRank for each node's most relevant neighborhood. DP-APPR protects nodes' edge information and limits sensitivity during DP-SGD training, enhancing nodes' feature information protection. Experiments on real-world graph datasets show our methods outperform existing ones in privacy-utility tradeoff. Future work includes developing tighter privacy DP-APPR algorithms and adaptive privacy budget strategies (e.g., between DP-APPR and DP-SGD based on dataset characteristics), as well as generalizing our approach to various types of graphs.

ACKNOWLEDGMENTS

This research was partially supported by the National Science Foundation (NSF) under CNS-2124104, CNS-2125530, CNS-2302968, IIS-2312502, NCS-2319449, and the National Institute of Health (NIH) under R01ES033241, R01LM013712, K25DK135913.

Appendix

Appendix

A PROOF FOR THEOREM 1

PROOF. We first consider the privacy loss of outputting the noisy APPR vector $\tilde{\mathbf{p}}_{(v_i)}$ for node v_i in Algorithm 1. For each element in the APPR vector, we use its value as its utility score. Since each element is nonnegative and clipped by the constant C_2 , the ℓ_1 sensitivity $\Delta(u)$ of each element is equal to C_2 . By adding the one-shot Gumbel noise $Gumbel(\beta\mathbf{1})$ where $\beta = C_2/\epsilon$ to the clipped APPR vector $\tilde{\mathbf{p}}_{(v_i)}$, option I selects K indices with the largest noisy values and satisfies (ϵ_1, δ) -DP where $\epsilon_1 = 2 \cdot \min\left\{K\epsilon, K\epsilon\left(\frac{e^{2\epsilon} - 1}{e^{2\epsilon} + 1}\right) + \epsilon\sqrt{2K \ln(1/\delta)}\right\}$ according to Corollary 1. Option II uses the Laplace mechanism [13] to report K selected noisy values. By adding Laplace noise $Laplace(KC_2/\epsilon_2)$ to each clipped element, option II costs an additional ϵ_2 privacy budget [13] since the ℓ_1 sensitivity of each element is C_2 , and satisfies $(\epsilon_1 + \epsilon_2, \delta)$ -DP.

Now we consider the privacy loss of Algorithm 1 which outputs M noisy APPR vectors. We use the optimal composition theorem in [22] which argues that for k sub-mechanisms, each with an (ϵ, δ) -DP guarantee, the overall privacy guarantee is (ϵ_g, δ_g) , where $\epsilon = \epsilon_g/(2\sqrt{k \ln(e + \epsilon_g/\delta_g)})$ and $\delta = \delta_g/2k$. By substituting M for k and $\epsilon_1/\epsilon_1 + \epsilon_2$ (option I/option II) for ϵ , the privacy loss of Algorithm 1 with option I is $(\epsilon_{g1}, 2M\delta)$, where $\epsilon_1 = \epsilon_{g1}/(2\sqrt{M \ln(e + \epsilon_{g1}/2M\delta)})$, and the privacy loss of Algorithm 1 with option II is $(\epsilon_{g2}, 2M\delta)$, where $\epsilon_1 + \epsilon_2 = \epsilon_{g2}/(2\sqrt{M \ln(e + \epsilon_{g2}/2M\delta)})$.

B GAUSSIAN MECHANISM (DP-APPR-GM)

We propose another DP APPR algorithm (DP-APPR-GM) based on the Gaussian mechanism [13] and output perturbation. DP-APPRGM utilizes a similar sampling and clipping strategy to limit the sensitivity of the APPR vector and directly adds Gaussian noise to each element to achieve DP. As shown in Algorithm 3, for each node v , we clip the ℓ_2

norm of its APPR vector $\mathbf{p}_{(v)}$ (line 6) and add the calibrated Gaussian noise to each element in the clipped $\mathbf{p}_{(v)}$ (line 8). We then select the top- K largest entries in $\tilde{\mathbf{p}}_{(v)}$ to get a sparse vector $\tilde{\mathbf{p}}_{(v)}$ (line 10).

Privacy Analysis of DP-APPR-GM.

Using the properties of the Gaussian mechanism and the optimal composition theorem [22], we establish the overall privacy guarantee for the DP-APPR-GM algorithm. Note that the DP guarantee is independent of K , in contrast with DP-APPR-EM.

THEOREM 3. *Let $\epsilon > 0$ and $\delta \in (0,1]$, Algorithm 3 is $(\epsilon_g, 2M\delta)$ -differentially private where $\epsilon = \epsilon_g / (2\sqrt{M \ln(e + \epsilon_g/2M\delta)})$.*

PROOF. We utilize the optimal composition theorem in [22] which argues that for k sub-mechanisms, each with an (ϵ, δ) -DP guarantee, the overall privacy guarantee is (ϵ_g, δ_g) -DP, where $\epsilon = \epsilon_g / (2\sqrt{k \ln(e + \epsilon_g/\delta_g)})$ and $\delta = \delta_g/2k$. In Algorithm 3, the noisy APPR vector for each node satisfies (ϵ, δ) -DP by the Gaussian mechanism independently. Since the returned APPR matrix contains the noisy APPR vectors of M nodes, the number of components for composition is M . We substitute M for k and $2M\delta$ for δ_g , which can conclude the proof.

C PROOF FOR THEOREM 2

PROOF. Denote μ_0 the Gaussian distribution with mean 0 and variance 1. Assume \mathbb{D}' is the neighboring feature dataset of \mathbb{D} , which differs at i^\dagger such that $x_{i^\dagger} \neq x_i$. Without loss of generality, we assume $\nabla f(\mathbf{x}_i) = 0$, for any $\mathbf{x}_i \in \mathbb{D}$, while $\nabla f(\mathbf{x}_{i^\dagger}) = \mathbf{e}_1$. Recall that the DP-APPR matrix is Π , where Π_i is the i -th row and the DP-APPR vector for node i , while $\Pi_{\cdot j}$ is the j -th column of Π . In addition, we can assume that $\|\Pi_{\cdot j}\|_1 \leq \tau$ due to the clipping in line 3, for all $j = 1, \dots, N$, and denote μ_τ the Gaussian distribution with mean τ and variance 1. Then, we have $\mathbb{E}[\mathcal{Z}(\mathbb{D})]$ and $\mathbb{E}[\mathcal{Z}(\mathbb{D}')]$ below,

$$\begin{aligned}
\mathbb{E}[\mathcal{Z}(\mathbb{D})] &= \left[\frac{|\mathcal{B}|}{N} \sum_{j \neq i^\dagger, j \notin \mathcal{N}(i^\dagger)} G_j \right] + \left[\frac{|\mathcal{B}|}{N} \sum_{j \neq i^\dagger, j \in \mathcal{N}(i^\dagger)} G_j \right] + \left[\frac{|\mathcal{B}|}{N} G_i \right] \\
&= \left[\frac{|\mathcal{B}|}{N} \sum_{j \neq i^\dagger, j \notin \mathcal{N}(i^\dagger)} \sum_{k \in \mathcal{N}(j)} \Pi_{jk} \nabla f(\mathbf{x}_k) \right] \\
&\quad + \left[\frac{|\mathcal{B}|}{N} \sum_{j \neq i^\dagger, j \in \mathcal{N}(i^\dagger)} \left(\sum_{k \in \mathcal{N}(j) \setminus i^\dagger} \Pi_{jk} \nabla f(\mathbf{x}_k) + \Pi_{ji^\dagger} \nabla f(\mathbf{x}_{i^\dagger}) \right) \right] \\
&\quad + \left[\frac{|\mathcal{B}|}{N} \left(\sum_{k \in \mathcal{N}(i^\dagger) \setminus i^\dagger} \Pi_{i^\dagger k} \nabla f(\mathbf{x}_k) + \Pi_{i^\dagger i^\dagger} \nabla f(\mathbf{x}_{i^\dagger}) \right) \right],
\end{aligned} \tag{5}$$

which indicates $\mathcal{Z}(\mathbb{D}) \sim \mu_0$.

$$\begin{aligned}
\mathbb{E}[\mathcal{G}(\mathbb{D}')] &= \left[\frac{|\mathcal{B}|}{N} \sum_{j \neq i^\dagger, j \notin \mathcal{N}(i^\dagger)} G_j \right] + \left[\frac{|\mathcal{B}|}{N} \sum_{j \neq i^\dagger, j \in \mathcal{N}(i^\dagger)} G_j' \right] + \left[\frac{|\mathcal{B}|}{N} G_i \right] \\
&= \left[\frac{|\mathcal{B}|}{N} \sum_{j \neq i^\dagger, j \notin \mathcal{N}(i^\dagger)} \sum_{k \in \mathcal{N}(j)} \mathbf{\Pi}_{jk} \nabla f(x_k) \right] \\
&\quad + \left[\frac{|\mathcal{B}|}{N} \sum_{j \neq i^\dagger, j \in \mathcal{N}(i^\dagger)} \left(\sum_{k \in \mathcal{N}(j) \setminus i^\dagger} \mathbf{\Pi}_{jk} \nabla f(x_k) + \mathbf{\Pi}_{ji} \nabla f(x_{i^\dagger}') \right) \right] \\
&\quad + \left[\frac{|\mathcal{B}|}{N} \left(\sum_{k \in \mathcal{N}(i^\dagger) \setminus i^\dagger} \mathbf{\Pi}_{ik} \nabla f(x_k) + \mathbf{\Pi}_{i i^\dagger} \nabla f(x_{i^\dagger}') \right) \right] \\
&= \mathbb{E}[\mathcal{G}(\mathbb{D})] + \frac{|\mathcal{B}|}{N} \sum_{j=1}^N \mathbf{\Pi}_{ji^\dagger} (f(x_{i^\dagger}') - f(x_j)) \\
&= \mathbb{E}[\mathcal{G}(\mathbb{D})] + \frac{|\mathcal{B}|}{N} \|\mathbf{\Pi}_{\cdot, i^\dagger}\|_1 \leq \mathbb{E}[\mathcal{G}(\mathbb{D})] + \frac{|\mathcal{B}|}{N} \tau,
\end{aligned} \tag{6}$$

which indicates $\mathcal{G}(\mathbb{D}') \sim \mu_0 + \frac{|\mathcal{B}|}{N} \mu_\tau$.

In the following, we quantify the divergence between \mathcal{G} and \mathcal{G}' by following the moments accountant [1], where we show that $\mathbb{E} \left[\left(\frac{\mu(z)}{\mu_0(z)} \right)^\lambda \right] \leq \alpha$, and $\mathbb{E} \left[\left(\frac{\mu_0(z)}{\mu(z)} \right)^\lambda \right] \leq \alpha$, for some explicit α .

To do so, the following is to be bounded for v_0 and v_1 .

$$\mathbb{E}_{z \sim v_0} \left[\left(\frac{v_0(z)}{v_1(z)} \right)^\lambda \right] = \mathbb{E}_{z \sim v_1} \left[\left(\frac{v_1(z)}{v_0(z)} \right)^{\lambda+1} \right] \tag{7}$$

Following [1], the above can be expanded with binomial expansion, which gives

$$\begin{aligned}
\mathbb{E}_{z \sim v_1} \left[\left(\frac{v_1(z)}{v_0(z)} \right)^{\lambda+1} \right] &= \sum_{t=0}^{\lambda+1} (\lambda+1) \mathbb{E}_{z \sim v_1} \left[\left(\frac{v_0 - v_1(z)}{v_1(z)} \right)^t \right] \\
&= 1 + 0 + T_3 + T_4 + \dots
\end{aligned} \tag{8}$$

Next, we bound T_3 by substituting the pairs of $v_0 = \mu_0, v_1 = \mu$ and $v_0 = \mu, v_1 = \mu_0$ in, and upper bound them, respectively.

For T_3 , with $v_0 = \mu_0, v_1 = \mu$, we have

$$\begin{aligned}
T_3 &= \frac{(\lambda+1)\lambda}{2} \mathbb{E}_{z \sim \mu} \left[\left(\frac{\mu_0(z) - \mu(z)}{\mu(z)} \right)^2 \right] = \frac{(\lambda+1)\lambda}{2} \mathbb{E}_{z \sim \mu} \left[\left(\frac{q\mu_r(z)}{\mu(z)} \right)^2 \right] \\
&= \frac{q^2(\lambda+1)\lambda}{2} \int_{-\infty}^{+\infty} \frac{(\mu_r(z))^2}{\mu_0(z) + q\mu_r(z)} dz \leq \frac{q^2(\lambda+1)\lambda}{2} \int_{-\infty}^{+\infty} \frac{(\mu_r(z))^2}{\mu_0(z)} dz \\
&= \frac{q^2(\lambda+1)\lambda}{2} \mathbb{E}_{z \sim \mu_0} \left[\left(\frac{\mu_r(z)}{\mu_0(z)} \right)^2 \right] = \frac{q^2(\lambda+1)\lambda}{2} \exp\left(\frac{\tau^2}{\sigma^2}\right) \\
&\leq \frac{q^2(\lambda+1)\lambda}{2} \left(\frac{\tau^2}{\sigma^2} + 1 \right) \leq \frac{q^2\tau^2(\lambda+1)\lambda}{\sigma^2},
\end{aligned} \tag{9}$$

where in the last inequality, we assume $\frac{\tau^2}{\sigma^2} + 1 \leq 2\frac{\tau^2}{\sigma^2}$, i.e., $\frac{\tau^2}{\sigma^2} \geq 1$. Thus, it requires $\sigma \leq \tau$.

As a result,

$$\alpha_{\mathcal{G}}(\lambda) \leq \frac{q^2\tau^2(\lambda+1)\lambda}{\sigma^2} + O(q^3\lambda^3/\sigma^3). \tag{10}$$

To satisfy $T \frac{q^2\tau^2\lambda^2}{\sigma^2} \leq \frac{\lambda\epsilon_{sgd}}{2}$, and $\exp\left(-\frac{\lambda\epsilon_{sgd}}{2}\right) \leq \delta_{sgd}$, we set

$$\epsilon_{sgd} = c_1 q^2 \tau^2 T, \tag{11}$$

$$\sigma = c_2 \frac{q\tau\sqrt{T\log(1/\delta_{sgd})}}{\epsilon_{sgd}}. \tag{12}$$

Given that the input DP-APPR matrix costs additional $(\epsilon_{pr}, \delta_{pr})$ privacy budget, by using the standard composition theorem of DP, the total privacy budget for the sampled graph G is $(\epsilon_{sgd} + \epsilon_{pr}, \delta_{sgd} + \delta_{pr})$. Since G is randomly sampled from the graph dataset \bar{G} , we can conclude the proof with the privacy amplification theorem of DP [5, 23].

Algorithm 3: DP-APPR using the Gaussian Mechanism (DP-APPR-GM)

Input: ISTA hyperparameters: γ, α, ρ ; privacy parameters: ϵ, δ ; clip bound C_1 , a graph (V, E) where $V = \{v_1, \dots, v_N\}$, an integer $K > 0$ and an integer $M \in [1, N]$.

- 1 **Initialize** the APPR matrix $\Pi \in \mathbb{R}^{M \times N}$ with all zeros.
- 2 **for** $i = 1, \dots, M$ **do**
- 3 **Compute APPR Vector:**
- 4 Compute the APPR vector $\mathbf{p}_{(v_i)}$ for node v_i using ISTA;
- 5 **Clip Norm:**
- 6 $\hat{\mathbf{p}}_{(v_i)} \leftarrow \mathbf{p}_{(v_i)} / \max\left(1, \frac{\|\mathbf{p}_{(v_i)}\|_2}{C_1}\right)$;
- 7 **Add Noise:**
- 8 $\tilde{\mathbf{p}}_{(v_i)} \leftarrow \hat{\mathbf{p}}_{(v_i)} + \mathcal{N}(0, \sigma^2 \mathbf{I})$, where $\sigma = \sqrt{2 \ln(1.25/\delta)} C_1 / \epsilon$;
- 9 **Sparsification:**
- 10 $\tilde{\mathbf{p}}'_{(v_i)} \leftarrow$: select the top K largest entries in $\tilde{\mathbf{p}}_{(v_i)}$ by setting all other entries with small values to zero.
- 11 **Replace** the i -th row of Π with $\tilde{\mathbf{p}}'_{(v_i)}$.
- 12 **end**
- 13 **return** Π and compute the overall privacy cost using the optimal composition theorem.

D DATASETS

We evaluate our method on five graph datasets: Cora-ML [6] which consists of academic research papers from various machine learning conferences and their citation relationships, Microsoft Academic graph [39] which contains scholarly data from various sources and the relationships between them, CS and Physics [39] which are co-authorship graphs, Reddit [19] which is constructed from Reddit posts, where edges represent connections between posts when the same user commented on both. Table 2 shows the statistics of the five datasets.

Table 2:

Dataset statistics

Dataset	Cora-ML	MS Academic	CS	Reddit	Physics
Classes	7	15	15	8	8
Features	2,879	6,805	6,805	602	8,415
Nodes	2,995	18,333	18,333	116,713	34,493
Edges	8,416	81,894	327,576	46,233,380	495,924

E ILLUSTRATION OF PRIVACY PROTECTION

To provide an intuitive illustration of the privacy protection provided by the DP trained models using our methods, we visualize the t-SNE clustering of training nodes' embeddings generated by the private models with varying ϵ values in Figure 9 for the Cora-ML dataset. We omit the results for other datasets as they display a similar pattern leading to the same conclusion. The color of each node corresponds to the label of the node. We can observe that when the privacy budget is small ($\epsilon = 1$), the model achieves strong privacy protection, thus it becomes hard to distinguish the training nodes belonging to different classes from each other. Meanwhile, when the privacy guarantee becomes weak

((ϵ) becomes larger), embeddings of nodes with the same class label are less obfuscated, hence gradually forming a cluster. This observation demonstrates that the privacy budget used in our proposed methods is correlated with the model's ability to generate private node embeddings, and therefore also associated with the privacy protection effectiveness against adversaries utilizing the generated embeddings to carry out privacy attacks [16, 27].

F MORE RESULTS ON EFFECTS OF PRIVACY PARAMETERS

Batch Size in DP-SGD (B).

Figure 10 shows batch size impact on model test accuracy. According to Theorem 2, with fixed privacy budget and epochs, Gaussian noise's standard deviation scales with the batch size's square root, increasing gradient noise for larger batches. However, larger batches may provide more accurate updates by encompassing more nodes and correlations. Thus, the curve remains relatively flat for batch sizes not too small.

Clipping Bound in DP-SGD (C).

Figure 11 shows the effect of gradient norm clipping bound C in DP-SGD on the model's test accuracy. The clipping bound affects the noise scale added to the gradients (linearly) as well as the optimization direction of model parameters. A large clipping bound may involve too much noise to the gradients, while a small clipping bound may undermine gradients' ability for unbiased estimation. The result verifies this phenomenon. We use $C = 1$ for all datasets in our experiments.

Number of Nodes in DP-APPR (M).

During the DP-APPR algorithm, a subset of M nodes is randomly sampled from the input training graph. Figure 12 illustrates the relationship between M and test accuracy under different total privacy budgets ($\epsilon = 1$ and $\epsilon = 8$, with $\delta = 2 \times 10^{-3}$). As M increases, the privacy budget allocated for calculating each DP-APPR vector decreases. This leads to more noise in each DP-APPR vector, which can adversely affect its utility and result in lower accuracy as observed. However, too small of an M will degrade the performance since it will not contain enough information about the graph structure. In our experiments, we set $M = 70$ for all datas.

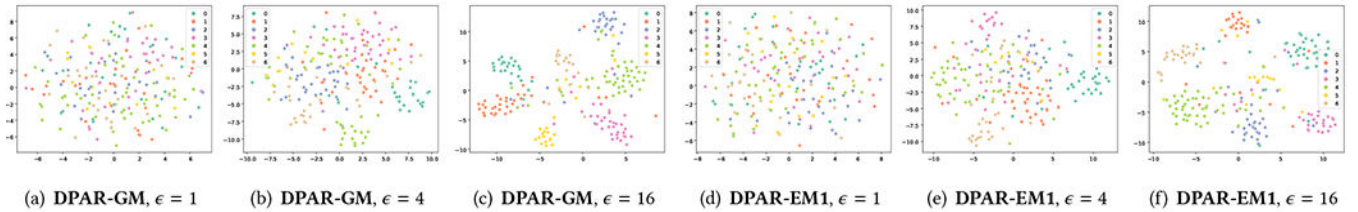


Figure 9:

Cora-ML. Clustering of training nodes' embeddings generated by private models with different privacy guarantees ϵ (fixed = 2×10^{-3}) and training methods.

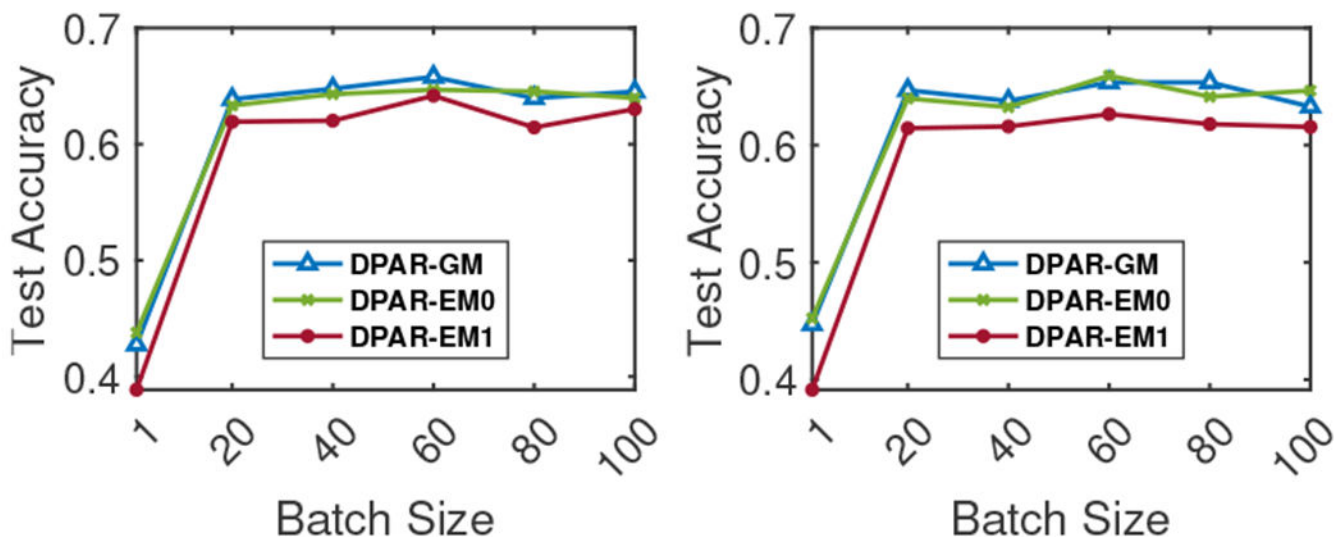


Figure 10:

Cora-ML. Batch size vs. model test accuracy. Fix total privacy budget $(\epsilon, \delta) = (8, 2 \times 10^{-3})$.

K=4 (left), K=16 (right)

G GENERALIZATION TO VARIOUS TYPES OF GRAPHS

DPAR proposed in this paper focuses on homogeneous graphs, including both homophilous and non-homophilous graphs, and can be applied in various domains such as social networks, recommendation systems, knowledge graphs, drug discovery, and traffic network analysis. Additionally, DPAR holds the potential for generalization to diverse graph types, including dynamic graphs, heterogeneous graphs, and those with high-dimensional features. For instance, in dynamic graphs, DPAR's decoupling strategy is well-regarded for its efficiency in addressing the high computational complexity often encountered in dynamic graph learning [20, 28]. Consequently, we can adapt the existing framework of DPAR by integrating established temporal differential privacy mechanisms [31, 33], which effectively manage specific challenges like temporal correlations among identical nodes across varying graph snapshots. In the context of heterogeneous graphs, prior research [33] demonstrates that homogeneous GNNs, like GCN and GAT, can process heterogeneous graphs by simply disregarding node and edge types. This finding suggests that extending DPAR to accommodate heterogeneous graphs, while concurrently implementing additional privacy safeguards for type information during type embedding learning, could yield favorable outcomes.

H COMPLEXITY OF DPAR

DPAR has linear computational complexity corresponding to the number of nodes and the node feature dimension. We elaborate as follows. In DP-APPR (Algorithm 1 and Algorithm 3), we calculate the APPR vector using ISTA [15]. Based on Theorem 3 in [15], the time complexity of ISTA for calculating the APPR vector depends only on the number of non-zeros of the calculated APPR vector, unlike calculations based on the entire graph. For

each APPR vector, the steps of clipping the norm, adding noise, and reporting noisy indexes have the worst-case time complexity that is linear to the number of nodes in the input graph. Since we calculate M DP-APPR vectors, the overall time complexity for DP-APPR algorithms is $O(MN) = O(N)(N \gg M)$ (N is the number of nodes), which indicates linear time complexity. In Algorithm 2, where we train the DP-GNN models using the node feature vectors and DP-APPR matrix, the model is a 2-layer MLP with each layer's size equal to 32. Therefore, the time complexity for each iteration is mainly bounded by the node feature dimension $D(D \gg 32)$. In conclusion, the overall time complexity for DPAR is $O(N + D)$, linearly related to the number of nodes and the node feature dimension.

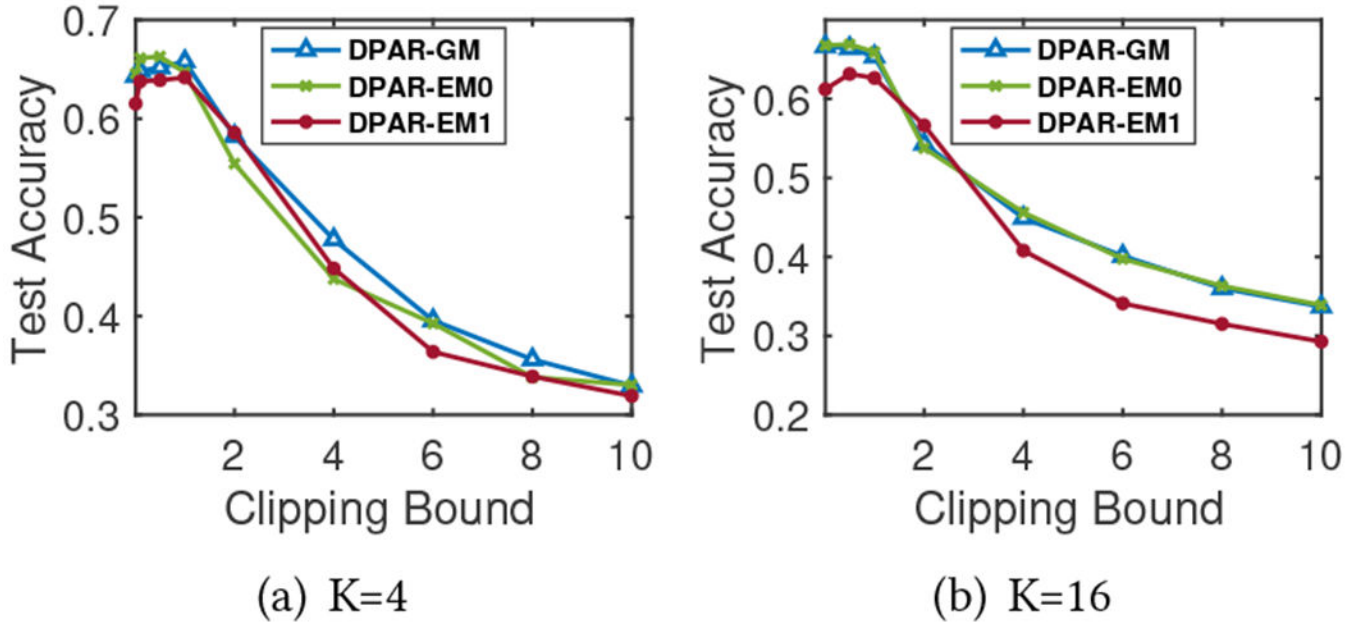


Figure 11: Cora-ML. Relationship between clipping bound of DP-SGD and model test accuracy. Fix total privacy budget $(\epsilon, \delta) = (8, 2 \times 10^{-3})$.

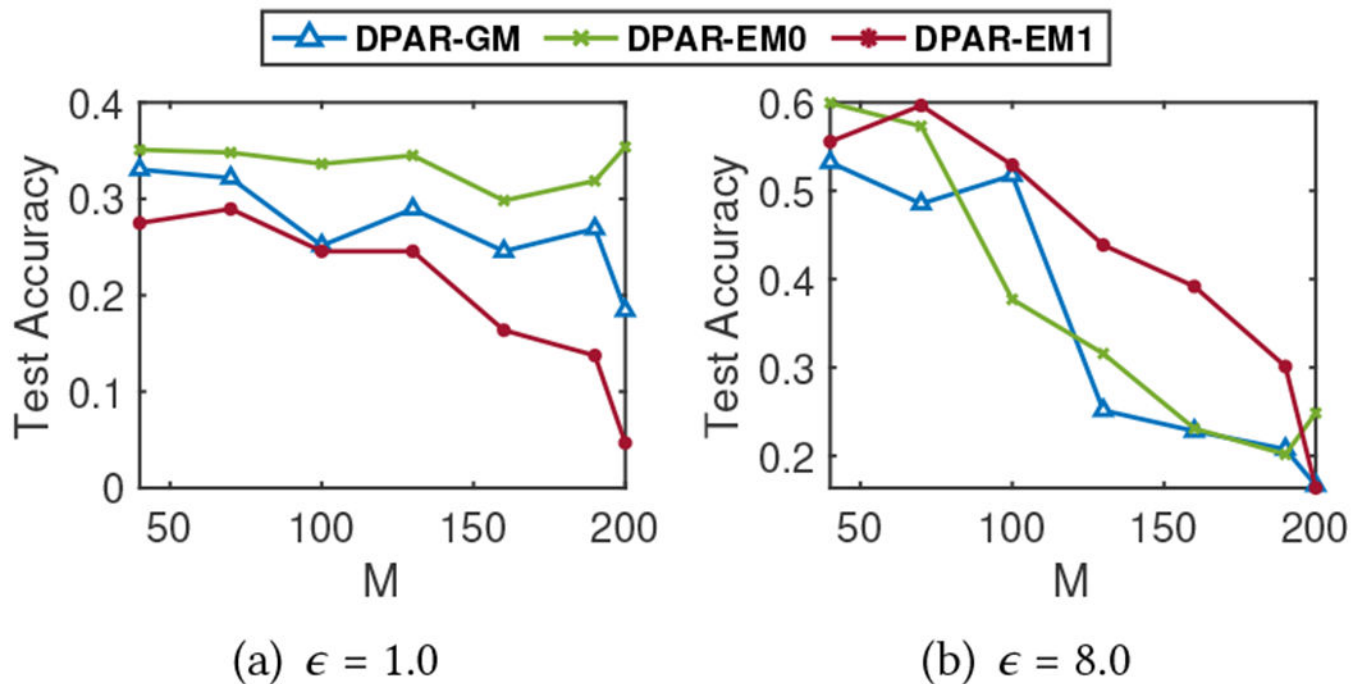


Figure 12: Cora-ML: Relationship between the number of nodes M in DP-APPAR vector calculation and model test accuracy. $K = 2$.

REFERENCES

- [1]. Abadi Martin, Chu Andy, Goodfellow Ian, McMahan H Brendan, Mironov Ilya, Talwar Kunal, and Zhang Li. 2016. Deep learning with differential privacy. In ACM SIGSAC CCS.
- [2]. Ahmed Faraz, Liu Alex X, and Jin Rong. 2019. Publishing Social Network Graph Eigenspectrum With Privacy Guarantees. *IEEE Transactions on Network Science and Engineering* 7, 2 (2019), 892–906.
- [3]. Andersen Reid, Chung Fan, and Lang Kevin. 2006. Local graph partitioning using pagerank vectors. In *FOCS 2006*. IEEE, 475–486.
- [4]. Bassily Raef, Smith Adam, and Thakurta Abhradeep. 2014. Differentially Private Empirical Risk Minimization: Efficient Algorithms and Tight Error Bounds. *arXiv:1405.7085 [cs.LG]*
- [5]. Beimel Amos, Brenner Hai, Kasiviswanathan Shiva Prasad, and Nissim Kobbi. 2014. Bounds on the sample complexity for private learning and private data release. *Machine learning* 94 (2014), 401–437.
- [6]. Bojchevski Aleksandar and Günnemann Stephan. 2018. Deep gaussian embedding of graphs: Unsupervised inductive learning via ranking. *ICLR* (2018).
- [7]. Bojchevski Aleksandar, Klicpera Johannes, Perozzi Bryan, Kapoor Amol, Blais Martin, Rózemerczki Benedek, Lukasik Michal, and Günnemann Stephan. 2020. Scaling graph neural networks with approximate pagerank. In *Proceedings of the 26th ACM SIGKDD International Conference on Knowledge Discovery & Data Mining*. 2464–2473.
- [8]. Chen Rui, Fung Benjamin CM, Philip S Yu, and Desai Bipin C. 2014. Correlated network data publication via differential privacy. *The VLDB Journal* 23, 4 (2014), 653–676.
- [9]. Daigavane Ameya, Madan Gagan, Sinha Aditya, Thakurta Abhradeep Guha, Aggarwal Gaurav, and Jain Prateek. 2021. Node-level differentially private graph neural networks. *arXiv preprint arXiv:2111.15521* (2021).

- [10]. Day Wei-Yen, Li Ninghui, and Lyu Min. 2016. Publishing graph degree distribution with node differential privacy. In Proceedings of the 2016 International Conference on Management of Data. 123–138.
- [11]. Dong Hande, Chen Jiawei, Feng Fuli, He Xiangnan, Bi Shuxian, Ding Zhaolin, and Cui Peng. 2021. On the Equivalence of Decoupled Graph Convolution Network and Label Propagation. The World Wide Web Conference (2021).
- [12]. Durfee David and Rogers Ryan M. 2019. Practical Differentially Private Top-k Selection with Pay-what-you-get Composition. Advances in Neural Information Processing Systems 32 (2019), 3532–3542.
- [13]. Dwork Cynthia, Roth Aaron, et al. 2014. The algorithmic foundations of differential privacy. Foundations and Trends[®] in Theoretical Computer Science 9, 3–4 (2014), 211–407.
- [14]. Epasto Alessandro, Mirrokni Vahab, Perozzi Bryan, Tsitsulin Anton, and Zhong Peilin. 2022. Differentially Private Graph Learning via Sensitivity-Bounded Personalized PageRank. arXiv preprint arXiv:2207.06944 (2022).
- [15]. Fountoulakis Kimon, Roosta-Khorasani Farbod, Shun Julian, Cheng Xiang, and Mahoney Michael W. 2019. Variational perspective on local graph clustering. Mathematical Programming 174, 1 (2019), 553–573.
- [16]. Fredrikson Matt, Jha Somesh, and Ristenpart Thomas. 2015. Model inversion attacks that exploit confidence information and basic countermeasures. In Proceedings of the 22nd ACM SIGSAC Conference on Computer and Communications Security. 1322–1333.
- [17]. Gao Tianchong and Li Feng. 2019. Sharing social networks using a novel differentially private graph model. In 2019 16th IEEE Annual Consumer Communications & Networking Conference (CCNC). IEEE, 1–4.
- [18]. Gleich David F. 2015. PageRank beyond the Web. siam REVIEW 57, 3 (2015), 321–363.
- [19]. Hamilton William L, Ying Rex, and Leskovec Jure. 2017. Inductive representation learning on large graphs. In Proceedings of the 31st International Conference on Neural Information Processing Systems.
- [20]. Hou Guanhao, Guo Qintian, Zhang Fangyuan, Wang Sibao, and Wei Zhewei. 2023. Personalized PageRank on Evolving Graphs with an Incremental Index-Update Scheme. Proceedings of the ACM on Management of Data 1, 1 (2023), 1–26.
- [21]. Jorgensen Zach, Yu Ting, and Cormode Graham. 2016. Publishing attributed social graphs with formal privacy guarantees. In Proceedings of the 2016 international conference on management of data. 107–122.
- [22]. Kairouz Peter, Oh Sewoong, and Viswanath Pramod. 2017. The Composition Theorem for Differential Privacy. IEEE Transactions on Information Theory 63, 6 (2017), 4037–4049.
- [23]. Kasiviswanathan Shiva Prasad, Lee Homin K, Nissim Kobbi, Raskhodnikova Sofya, and Smith Adam. 2011. What can we learn privately? SIAM J. Comput 40, 3 (2011), 793–826.
- [24]. Kasiviswanathan Shiva Prasad, Nissim Kobbi, Raskhodnikova Sofya, and Smith Adam. 2013. Analyzing graphs with node differential privacy. In Theory of Cryptography Conference. Springer, 457–476.
- [25]. Klicpera Johannes, Bojchevski Aleksandar, and Günnemann Stephan. 2019. Predict then propagate: Graph neural networks meet personalized pagerank. ICLR (2019).
- [26]. Lee Jaewoo and Kifer Daniel. 2018. Concentrated differentially private gradient descent with adaptive per-iteration privacy budget. In KDD.
- [27]. Li Kaiyang, Luo Guangchun, Ye Yang, Li Wei, Ji Shihao, and Cai Zhipeng. 2020. Adversarial Privacy Preserving Graph Embedding against Inference Attack. IEEE Internet of Things Journal (2020).
- [28]. Li Yiming, Shen Yanyan, Chen Lei, and Yuan Mingxuan. 2023. Zebra: When Temporal Graph Neural Networks Meet Temporal Personalized PageRank. Proceedings of the VLDB Endowment 16, 6 (2023), 1332–1345.
- [29]. Lin Wanyu, Li Baochun, and Wang Cong. 2022. Towards Private Learning on Decentralized Graphs with Local Differential Privacy. arXiv:2201.09398 (2022).
- [30]. Liu Meng, Gao Hongyang, and Ji Shuiwang. 2020. Towards deeper graph neural networks. In 26th ACM SIGKDD. 338–348.

- [31]. Liu Xiyang, Kong Weihao, Jain Prateek, and Oh Sewoong. 2022. DP-PCA: Statistically Optimal and Differentially Private PCA. *Advances in Neural Information Processing Systems* 35 (2022), 29929–29943.
- [32]. Lu Wentian and Miklau Gerome. 2014. Exponential random graph estimation under differential privacy. In *Proceedings of the 20th ACM SIGKDD international conference on Knowledge discovery and data mining*. 921–930.
- [33]. Lv Qingsong, Ding Ming, Liu Qiang, Chen Yuxiang, Feng Wenzheng, He Siming, Zhou Chang, Jiang Jianguo, Dong Yuxiao, and Tang Jie. 2021. Are we really making much progress? revisiting, benchmarking and refining heterogeneous graph neural networks. In *Proceedings of the 27th ACM SIGKDD conference on knowledge discovery & data mining*. 1150–1160.
- [34]. Ma Jing, Zhang Qiuchen, Lou Jian, Ho Joyce C, Xiong Li, and Jiang Xiaoqian. 2019. Privacy-preserving tensor factorization for collaborative health data analysis. In *Proceedings of the 28th ACM International Conference on Information and Knowledge Management*. 1291–1300.
- [35]. Maurya Sunil Kumar, Liu Xin, and Murata Tsuyoshi. 2022. Simplifying approach to node classification in Graph Neural Networks. *Journal of Computational Science* 62 (2022), 101695.
- [36]. Nguyen Hiep H, Imine Abdessamad, and Rusinowitch Michaël. 2015. Differentially private publication of social graphs at linear cost. In *2015 IEEE/ACM International Conference on Advances in Social Networks Analysis and Mining (ASONAM)*. IEEE, 596–599.
- [37]. Sajadmanesh Sina and Gatica-Perez Daniel. 2021. Locally private graph neural networks. In *Proceedings of the 2021 ACM SIGSAC Conference on Computer and Communications Security*. 2130–2145.
- [38]. Sajadmanesh Sina, Shamsabadi Ali Shahin, Bellet Aurélien, and Gatica-Perez Daniel. 2023. GAP: Differentially Private Graph Neural Networks with Aggregation Perturbation. In *32nd USENIX Security Symposium*.
- [39]. Shchur Oleksandr, Mumme Maximilian, Bojchevski Aleksandar, and Günnemann Stephan. 2018. Pitfalls of graph neural network evaluation. *Relational Representation Learning Workshop (R2L 2018), NeurIPS (2018)*.
- [40]. Wu Bang, Yang Xiangwen, Pan Shirui, and Yuan Xingliang. 2021. Adapting membership inference attacks to GNN for graph classification: approaches and implications. In *2021 IEEE International Conference on Data Mining (ICDM)*. IEEE, 1421–1426.
- [41]. Wu Zonghan, Pan Shirui, Chen Fengwen, Long Guodong, Zhang Chengqi, and Philip S Yu. 2020. A comprehensive survey on graph neural networks. *IEEE transactions on neural networks and learning systems* (2020).
- [42]. Xiao Qian, Chen Rui, and Tan Kian-Lee. 2014. Differentially private network data release via structural inference. In *Proceedings of the 20th ACM SIGKDD international conference on Knowledge discovery and data mining*. 911–920.
- [43]. Yang Carl, Wang Haonan, Sun Lichao, and Li Bo. 2020. Secure Network Release with Link Privacy. *arXiv:2005.00455* (2020).
- [44]. Zhang Jun, Cormode Graham, Procopiu Cecilia M, Srivastava Divesh, and Xiaokui Xiao. 2015. Private release of graph statistics using ladder functions. In *Proceedings of the 2015 ACM SIGMOD international conference on management of data*. 731–745.
- [45]. Zhang Jun, Zhang Zhenjie, Xiao Xiaokui, Yang Yin, and Winslett Marianne. 2012. Functional Mechanism: Regression Analysis under Differential Privacy. *Proceedings of the VLDB Endowment* 5, 11 (2012).
- [46]. Zhang Qiuchen, Ma Jing, Lou Jian, and Xiong Li. 2021. Private stochastic non-convex optimization with improved utility rates. In *Proceedings of the Thirtieth International Joint Conference on Artificial Intelligence*.
- [47]. Zhang Qiuchen, Ma Jing, Xiao Yonghui, Lou Jian, and Xiong Li. 2020. Broadening differential privacy for deep learning against model inversion attacks. In *2020 IEEE International Conference on Big Data (Big Data)*. IEEE, 1061–1070.
- [48]. Zhang Shijie, Yin Hongzhi, Chen Tong, Huang Zi, Cui Lizhen, and Zhang Xiangliang. 2021. Graph Embedding for Recommendation against Attribute Inference Attacks. *arXiv:2101.12549* (2021).

- [49]. Zhang Zhikun, Chen Min, Backes Michael, Shen Yun, and Zhang Yang. 2022. Inference attacks against graph neural networks. In 31st USENIX Security Symposium (USENIX Security 22). 4543–4560.
- [50]. Zhang Zaixi, Liu Qi, Huang Zhenya, Wang Hao, Lu Chengqiang, Liu Chuanren, and Chen Enhong. 2021. Graphmi: Extracting private graph data from graph neural networks. arXiv preprint arXiv:2106.02820 (2021).

Author Manuscript

Author Manuscript

Author Manuscript

Author Manuscript

CCS CONCEPTS

- Security and privacy → Privacy protections;
- Computing methodologies → Neural networks.

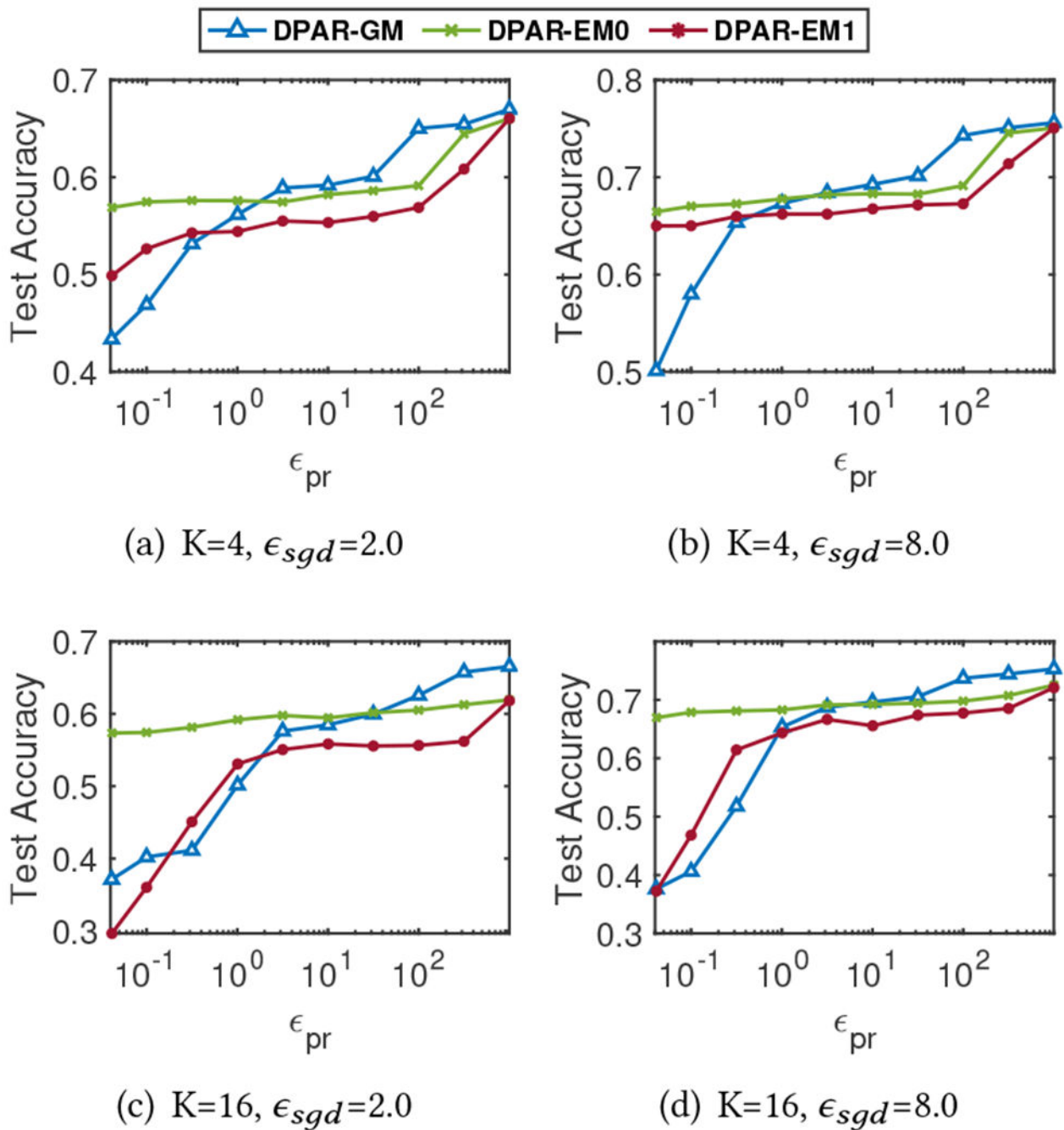


Figure 1:
Relationship between privacy budget ϵ (fixed $\delta = 2 \times 10^{-3}$) and test accuracy on Cora-ML dataset.

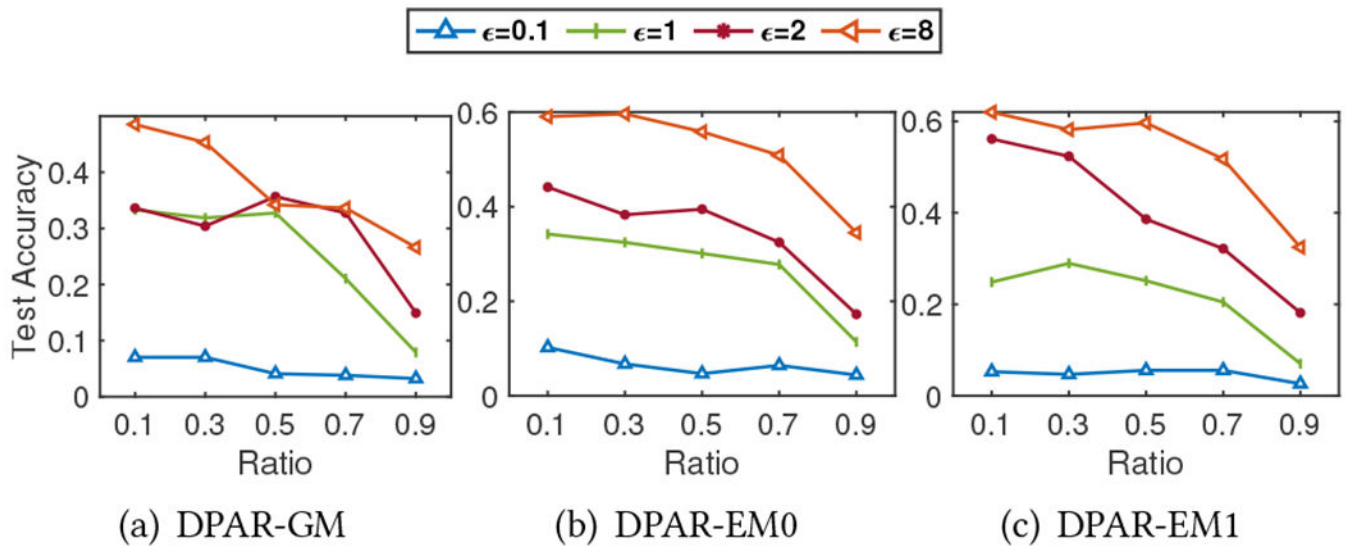


Figure 2:
Cora-ML. The privacy budget ϵ ratio for DP-ARRP

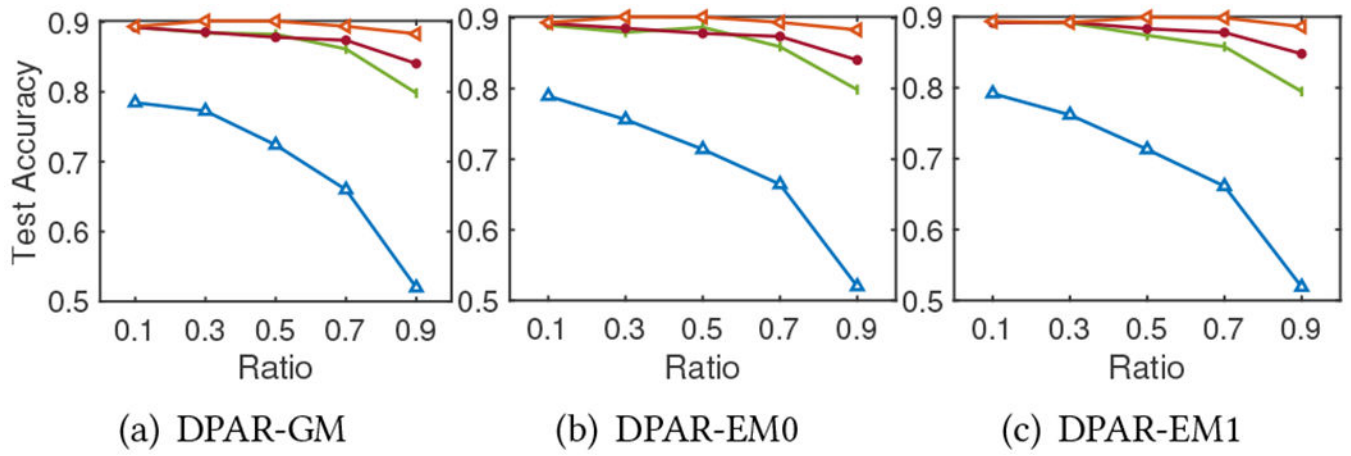


Figure 3:
CS. The privacy budget ϵ ratio for DP-ARRP

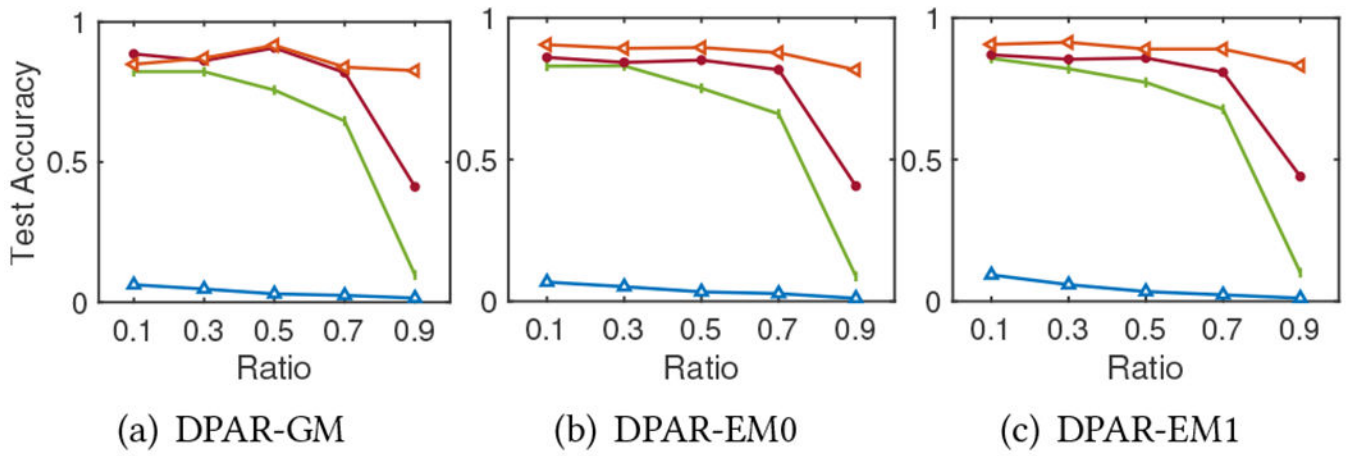


Figure 4:
MS Academic. The privacy budget ϵ ratio for DP-ARRP

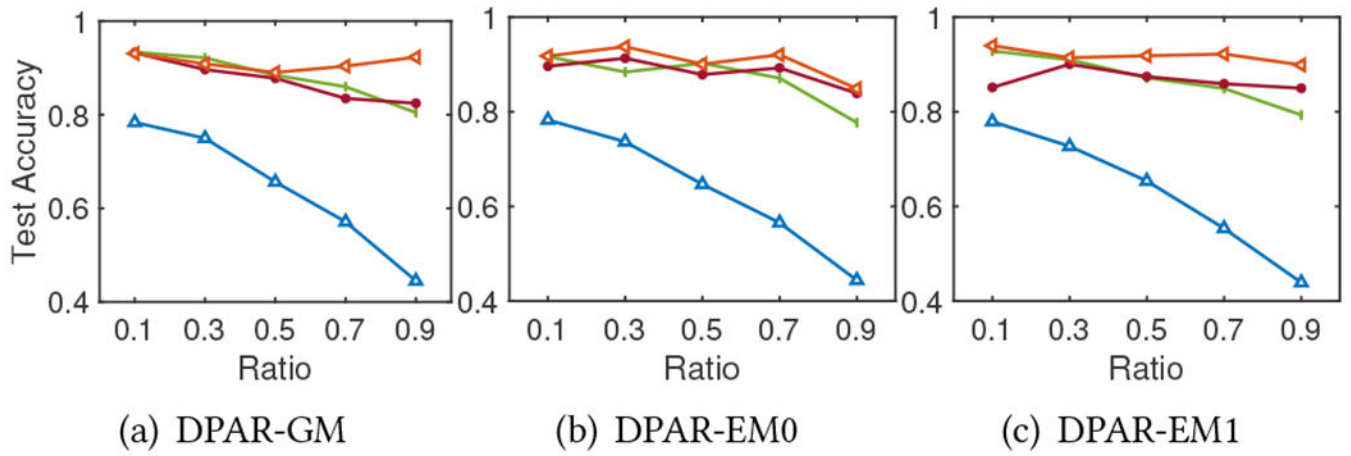


Figure 5:
 Reddit. The privacy budget ϵ ratio for DP-ARRP

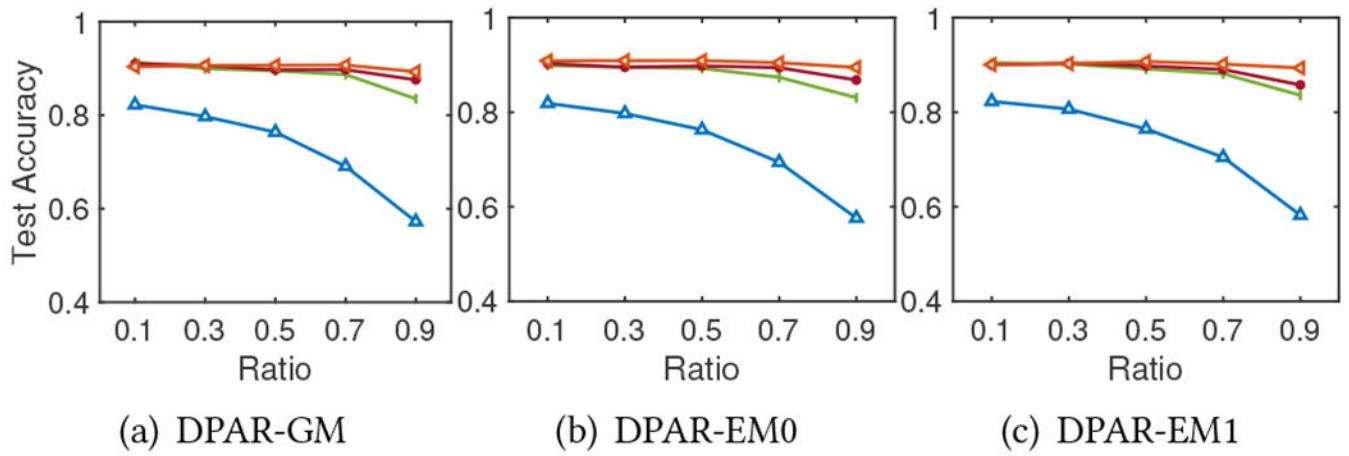
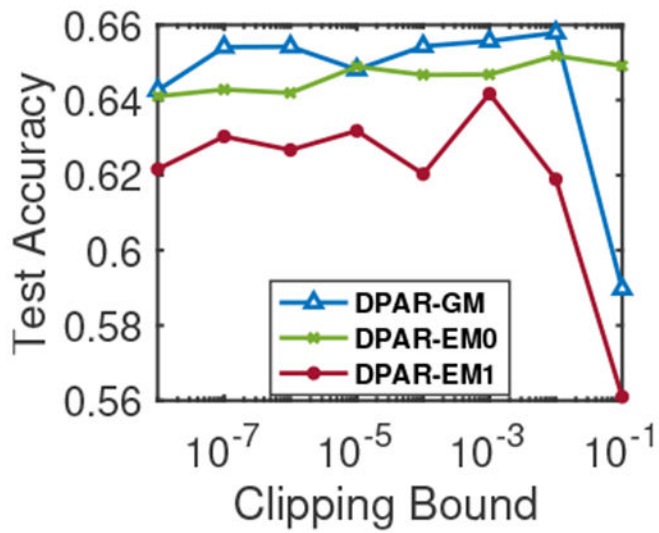
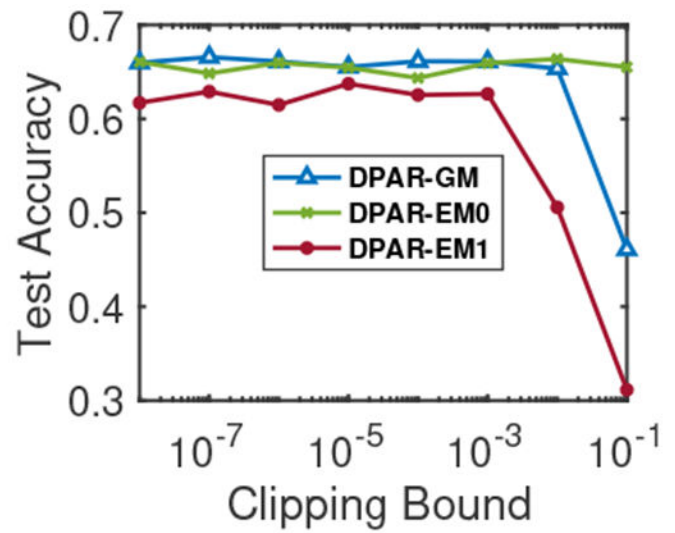


Figure 6:
Physics. The privacy budget ϵ ratio for DP-ARRP



(a) K=4



(b) K=16

Figure 7: Cora-ML. Relationship between clipping bound of DP-APPR and model test accuracy. Total privacy $(\epsilon, \delta) = (8, 2 \times 10^{-3})$.

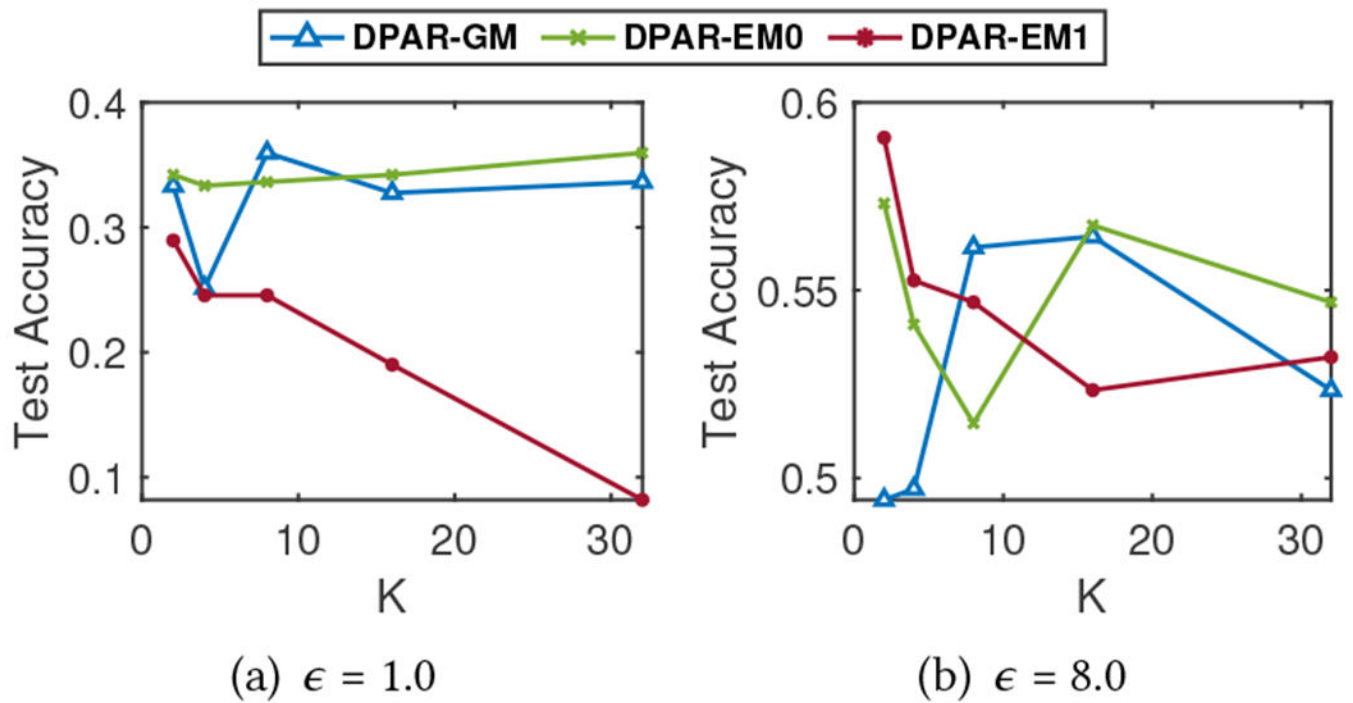


Figure 8:
Cora-ML: Relationship between the number of top- K entries in DP-APPR vector and model test accuracy.

Table 1:

Privacy budget and test accuracy on each graph dataset

Dataset	Privacy (ϵ, δ)	GAP	SAGE	Features	DPAR-EM0	DPAR-EMI	DPAR-GM	DPARNoDP	GAPNoDP	FeaturesNoDP
Cora-ML	$(1, 2 \times 10^{-3})$ $(8, 2 \times 10^{-5})$	0.34	0.152	0.5733	0.3421	0.2895	0.3333	0.7076	0.8883	0.7733
		0.5733	0.368	0.6107	0.5965	0.6199	0.4854			
MS Academic	$(1, 8 \times 10^{-4})$ $(8, 8 \times 10^{-4})$	0.6563	0.013	0.83	0.8306	0.8569	0.8225	0.955	0.9571	0.8382
		0.8581	0.063	0.8723	0.9054	0.9135	0.9165			
CS	$(1, 8 \times 10^{-4})$ $(8, 8 \times 10^{-4})$	0.66	0.0917	0.8344	0.8898	0.8921	0.8927	0.9707	0.9571	0.9307
		0.8537	0.7366	0.895	0.9017	0.8994	0.9063			
Reddit	$(1, 1 \times 10^{-4})$ $(8, 1 \times 10^{-4})$	0.7047	0.086	0.7436	0.9167	0.9286	0.934	0.9698	0.9949	0.8337
		0.9161	0.82	0.777	0.9375	0.9399	0.931			
Physics	$(1, 1 \times 10^{-4})$ $(8, 1 \times 10^{-4})$	0.8192	0.1263	0.8412	0.8887	0.8927	0.8948	0.9548	0.9597	0.9504
		0.9088	0.8919	0.9017	0.9023	0.9020	0.9101			